1968

Computer simulation of radiation damage in Fe_3Al

Roland Otto Jackson

Department:

COMPUTER SIMULATION OF RADIATION DAMAGE IN Fe_3Al

by

ROLAND OTTO JACKSON, 1944

A

THESIS

submitted to the faculty of

THE UNIVERSITY OF MISSOURI AT ROLLA

in partial fulfillment of the requirements for the

Degree of

MASTER OF SCIENCE IN NUCLEAR ENGINEERING

Rolla, Missouri

1968

Approved by

H. P. Leighly Jr. (advisor) D. E. Edwards

Otto H. Hill

ABSTRACT

A computer program, designed to simulate the ordered state of the B.C.C. alloy, Fe_3Al, was used to study the effects of irradiation on an order-disorder alloy.

Twenty-six runs were made with this program representing a variety of initial conditions. In all cases, the final damaged state consisted of Frenkel defects, vacancy-interstitial pairs; and the distance separating these pairs was a sensitive function of the energy and direction imparted to the primary knock-on. Both the vacancy and the interstitial were found to be normal, stable defects, with the interstitial residing in a "split"-configuration oriented in the [110] direction.

The threshold energies for permanent atomic displacement were also found to be strongly directionally dependent. The [100] direction proved to have the lowest threshold with a value of 22 eV (for a chain of all Fe atoms) for the directions studied. The threshold for the [110] direction was about 44 eV, while that for the [111] direction was not determined because of its very complex behavior.

"Replacement chains" were prevalent in the [100] and the [110] directions. After an initial energy loss of about 10 to 15 eV, the replacement chains progressed with

relatively little loss of energy per atomic collision.

"Focusons" were also prevalent and served as the primary mechanism for dissipating energy from the collision chain. This mechanism was operative in the [100] and [111] directions and was especially noticeable during the "defocusing" collisions.

The defocusing replacement chains were introduced at energies of about 110 eV and knock-on directions from 1 to 1.5° away from the [100] and [111] directions. The energy dissipation along a defocused chain closely resembled the "thermal spike" concept; while, the extensive expansion of the lattice near the end of the defocused chain (especially in the [111] direction) was reminiscent of a "plasticity spike."

The presence of aluminum atoms had a strong influence on several of the dynamic events. The small mass of the aluminum atoms present in the [111] chain impeded the progress of the replacement chain; while, the defocusing in the [100] and [111] directions was enhanced by the aluminum's low mass and high mobility.

Disordering was found to be most significant in the defocused chains. The [100] and [110] replacement chains containing all iron atoms showed no disordering when the iron atoms exchanged places. Since the aluminum atoms were not replaced in either the [111] direction or the [100] (alternate iron and aluminum atoms) direction, no

disordering occurred. The disordering in the defocused chains arose from the general mixing of the lattice atoms along the chain and especially in the "plasticity spike" region.

ACKNOWLEDGMENT

The author wishes to gratefully thank both Dr. H. P. Leighly, Associate Professor of Metallurgical Engineering, for his advice and suggestions with regard to the metallurgical aspects of this research, and Dr. D. R. Edwards, Director of the Nuclear Reactor, for his valuable assistance in the preparing of the computer program used.

The author would like to thank the U.M.R. Computer Science Center for generously furnishing the computer facilities, and the U.S. Atomic Energy Commission under whose traineeship the author was able to do this research.

In addition, the author wishes to express his sincere appreciation to his wife, Kathy, whose valuable support and assistance in the preparation of this thesis insured its completion.

TABLE OF CONTENTS

TABLE OF CONTENTS (cont'd)

LIST OF FIGURES

LIST OF FIGURES (cont'd)

Chapter I

INTRODUCTION

For the past twenty years a great deal of work has gone into the investigation of the effects of irradiation on materials. The interest in this subject has arisen from the observation of significant physical property changes that occurred after materials had been exposed to large dosages of neutron radiation ($\sim 10^{20}$nvt). The effects induced in metals and alloys have been of particular interest as most nuclear reactor components and associated structures were metallic in nature. The importance of metal behavior under conditions of irradiation was brought to light by the occurrence of gross structural failures; especially, the failure of a number of reactor pressure vessels. The need to insure safe nuclear reactor operation resulted in a flurry of testing of the effects of radiation on specific materials to be used in the construction of nuclear facilities.

The obvious shortcomings of this approach were soon realized and efforts were begun to study the more basic mechanisms involved in radiation damage. It was felt that a knowledge of the damage mechanism, operating in certain pure metals and alloys of different structures and composi-

tions, could be extrapolated to predict property changes in any other metal or alloy.

One of the most promising approaches to date involved a high speed computer used to simulate, numerically, the damage produced by a single knock-on of moderate energy (10 to 100 eV) in a lattice of any desired configuration.

The purpose of this thesis is to present the results of investigations carried out with such a computer program designed to represent the body centered cubic, ordered alloy, Fe_3Al.

Chapter II

REVIEW OF LITERATURE

Before entering into an explanation of the experimental procedure and results, some background is needed into the structure and properties of Fe_3Al, and, of special interest, the results of irradiation damage experiments performed, to date, on order-disorder alloys in general.

A. The Ordered Alloy System

For a long time, it was assumed that the placement of atoms on lattice sites during the formation of a binary substitutional solid solution resulted in a completely random arrangement of solvent and solute atoms on the lattice sites. That this might not always be the case was first postulated from chemical properties by Tammann in 1919 (1); however, the strongest evidence was furnished by the presence of superstructure lines on X-ray diffraction patterns, observed first in CuAu by Johansson and Linde (2) in 1925. If the composition of an alloy could be expressed in a stochiometrically simple formula AB or A_3B (or, at least, very near to these ratios) then it was possible for the atoms to occupy specific sites on the lattice, and the structure was said to be "ordered." When an alloy had become ordered throughout

some "domain," it was said to have developed a "superlattice."

In some binary systems, such as copper and gold, the chemical activities of the solid solutions exhibit negative deviations (3). These deviations were often considered as evidence that unlike atoms had a definite attraction for one another; or, at least, a preference for neighbors of a different atomic species. An interesting result of this effect occurred in the copper-gold system where the atoms alternate on the lattice sites in such a way as to form the maximum number of unlike atomic bonds (Cu-Au) and the minimum number of like bonds (either Cu-Cu or Au-Au). Under these circumstances the gold atoms had a statistically larger number of copper nearest neighbors than random occurrence would dictate. At elevated temperatures, thermal motion was too great to allow the formation of large numbers of atoms into ordered structures. As the temperature was elevated, thermal vibrations increased until some atoms possessed sufficient kinetic energy to break their lattice bonds and exchange positions with neighboring atoms. The breaking of unlike bonds and the formation of more like bonds was energetically unfavorable and increased the free energy of the system, introducing a driving force to re-order the system. The two opposing factors, namely, the attraction of unlike atoms for each other and disrupting influence of thermal motion, led to the condition known as "short range"

order.

On heating to a sufficiently high temperature, called the "critical temperature," the superlattice disappeared rather sharply with the loss of long range order; while, a certain amount of short range order always existed due to the attraction of unlike atoms. The disappearance of the superlattice bore a strong resemblance to a solid lattice on melting. Since at the critical temperature, the ordered state was still energetically more favorable than the disordered state, energy had to be supplied to destroy the superlattice much as the heat of fusion was needed to melt the solid. Unlike the isothermal energy absorption associated with the heat of fusion, the energy used in destroying the superlattice was absorbed over a range of temperatures below the critical temperature, and appeared as an increase in the heat capacity in this range.

Another factor that often aided the formation of an ordered state was a difference in size between the atomic species involved. Darken and Gurry (4) have indicated that an ordered structure could most easily accommodate a difference in atomic radii. There was a limit, however, to the size difference for which the ordered state could exist, as was evident in the B.C.C. (body-centered cubic) structure when the body center sphere was so small that it could not be tangent to all the corner spheres simultaneously even though they were all in contact with one another in the

densest arrangement.

The iron-aluminum system, see Figure 1 (from Hansen and Anderko (5)), involved a complicated set of superlattice arrangements. Bradley and Jay (6) had investigated this system thoroughly using X-ray diffraction techniques and found that in the range 0 to 25 atom per cent aluminum no superlattice, or long range order, was detectable. In the range 25 to 50 atom per cent, a superlattice structure was evident that existed even after the alloys were quenched in the same manner often employed to disorder ordered alloys.

As the aluminum content was increased above 25 per cent, the degree of order was increased and there was a continuous change in the lattice parameters. This provided clear evidence that an ordered structure allowed a better atom fit and a more dense structure. It was interesting to note that, although the coordination number for B.C.C. was 8, each atom had six second near neighbors that were just slightly farther away than the 8 nearest neighbors. The iron-aluminum system with 25 atomic per cent aluminum (Fe_3Al) did not form in the same way that other common A_3B alloys such as Cu_3Au form. Darken and Gurry (4) noted that the F.C.C. structure was more amenable to an alloy with an atomic ratio of 3:1, while the B.C.C. structure was particularly suited to a 1:1 ratio. The unusual occurrence of Fe_3Al (see Figure 2) as a B.C.C. structure was explained by Darken and Gurry as arising from the fairly large difference in electronegativity

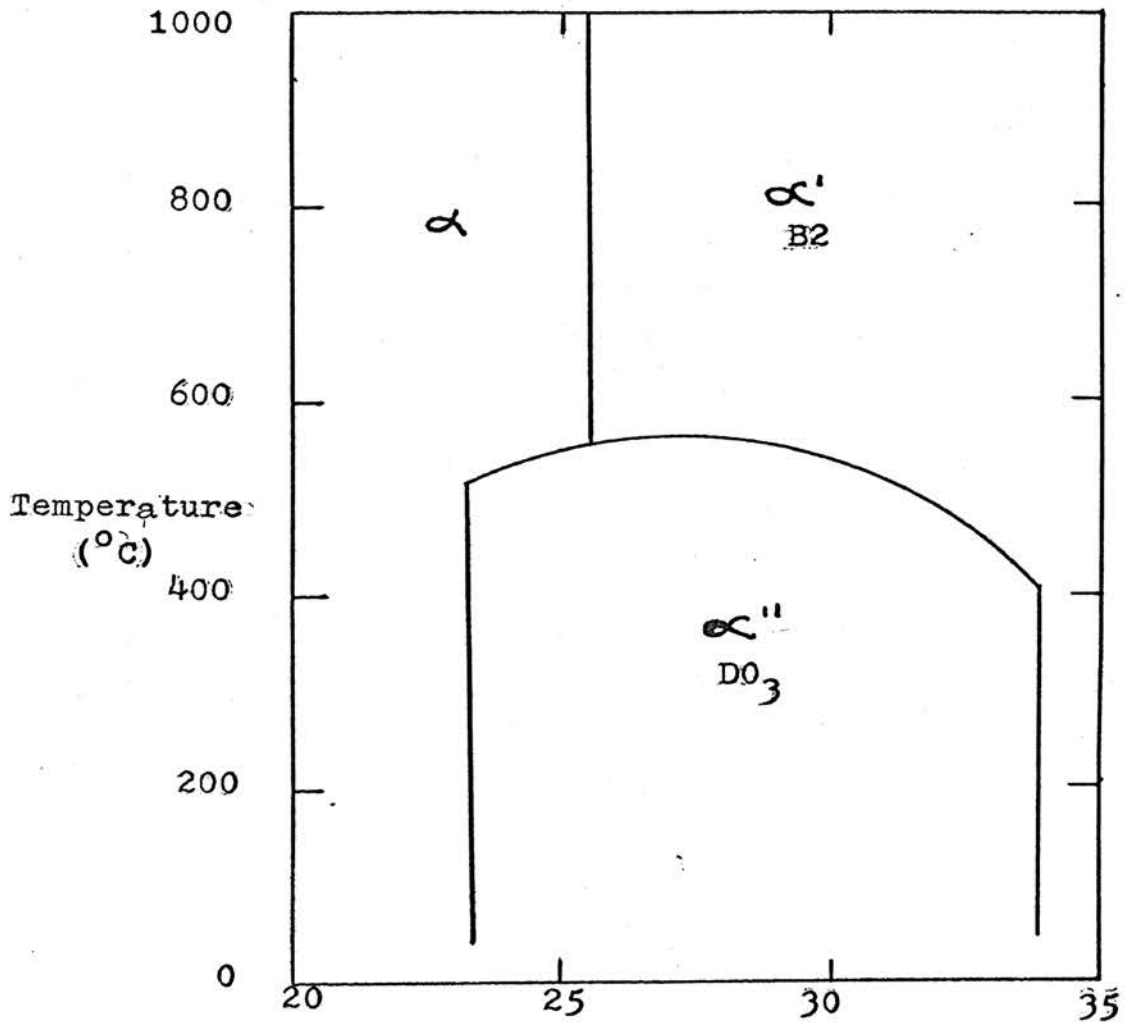

Iron-Aluminum Equilibrium Diagram, (5)

Figure 1

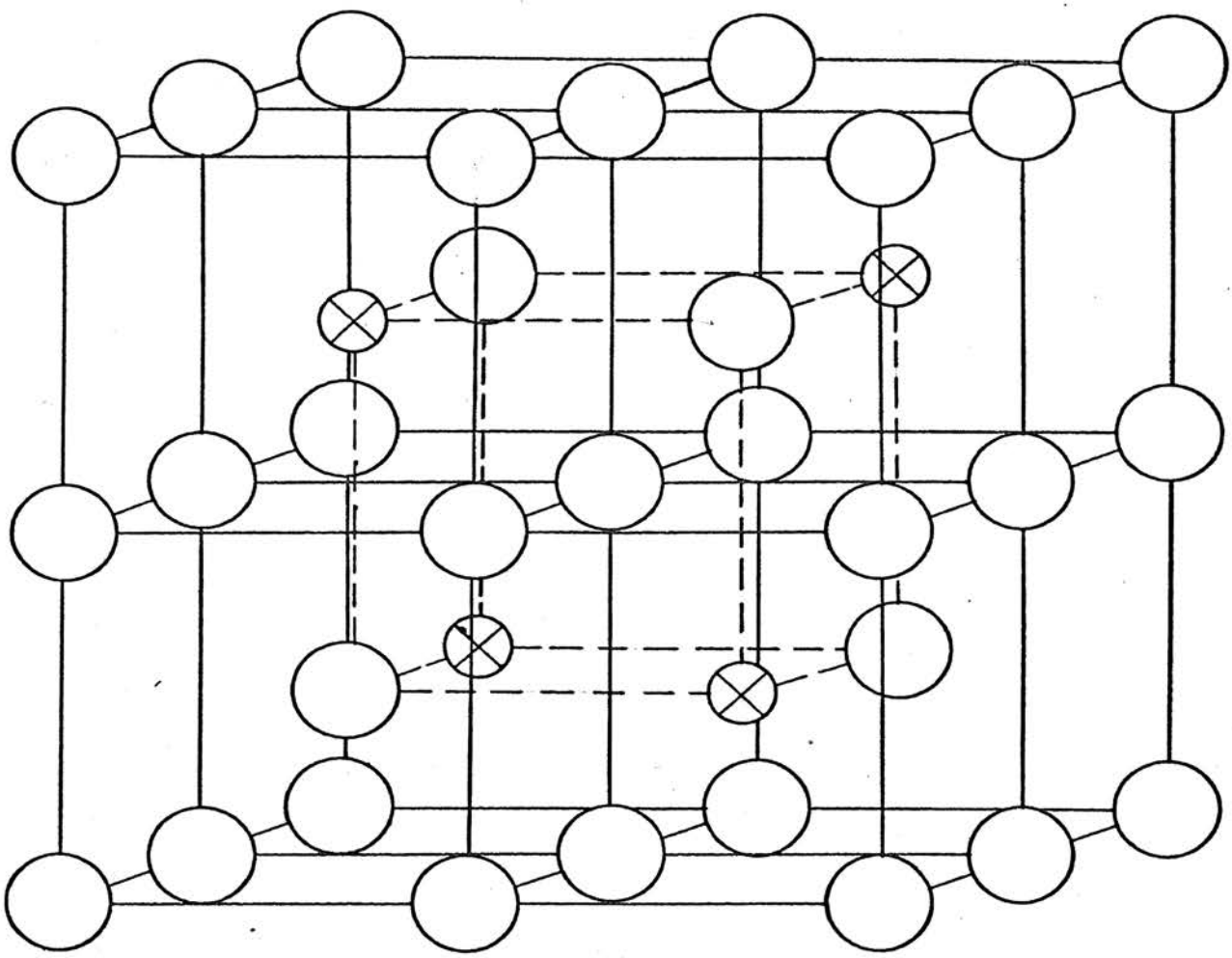

Iron

Aluminum

Fe_3Al (DO_3) Superlattice

Figure 2

between iron and aluminum. Mott and Jones (7) concluded from this that the aluminum atoms could have no aluminum nearest neighbors, and, in fact, they have no aluminum as second nearest neighbors in the Fe_3Al structure. Half the lattice points, those that lie on one simple cubic lattice, were permanently occupied by Fe atoms. This alloy thus behaved, with respect to the development of order, as an AB (1:1) alloy. Energy considerations were satisfied since a lower energy state exists when an aluminum atom had all dissimilar neighbors.

B. Radiation Damage on Order-Disorder Alloys

Initially, studies of order-disorder alloys were for purely academic reasons; however, it soon became apparent that certain physical and mechanical properties, such as electrical resistivity, magnetic susceptibility, and hardness, were sensitive functions of the degree of order present. Quantum mechanical calculations indicated that the electrical resistivity of a completely ordered state should be zero while that of the opposite, completely disordered state, should be infinite. Although this ideal case only held in theory, there existed, in many alloys, a marked decrease in the resistivity of the alloy as it went from a disordered to an ordered state. It was soon realized that these property changes might well furnish an external measure of the rearrangement of lattice atoms which would go

unobserved in most pure metals and alloys.

The important part order-disorder alloys have played in radiation damage studies had arisen from the sensitivity of property changes to fast particle irradiation. This sensitivity existed because order-disorder alloys differed from random alloys and pure metals in the following ways (8):

a) Changes that resulted from displaced atoms might be observed even after the displaced atoms had returned to lattice sites, since they might be expected to return in a random manner and, thus, leave the degree of order altered. Similarly, any exchange of atoms induced by radiation, unobservable in pure metals and random alloys, resulted in an altered degree of order.

b) Several of the physical and mechanical properties of order-disorder alloys were very sensitive to the degree of order, and made a useful tool for quantitative determinations of the magnitude of radiation damage.

When a fast particle traversed a lattice, it might lose energy by one of several methods; however, for the purpose of this study the most important of these will be that which led to the displacement of a lattice atom to form a Frenkel defect; that is a vacancy-interstitial pair. This energy loss occurred through elastic collisions between the moving particle and the stationary atoms. According to Billington and Crawford (9), if in an elastic collision the energy, E_p,

transferred to a stationary atom was greater than some threshold, E_d (Wigner energy), then the stationary atom would be displaced from its normal lattice site and, most often, would come to rest in a non-equilibrium or interstitial site. Threshold values of 10 to 30 eV for monatomic solids had been reported. This value was about five times the energy for thermal generation of Frenkel defects, because the displacement occurred before the surrounding lattice had had a chance to relax. The process described above, where the fast particle displaced a lattice atom was called the "primary process" and the atom that was displaced was called the "knock-on." If the energy of the "knock-on," E_p, was much greater than E_d then the "knock-on" might assume the role of the projectile and cause secondary and tertiary displacements.

The above process of defect formation should not be construed as the only process. This simple theory does not provide for the multitude of other mechanisms that have since been proposed to explain the results of radiation damage studies. Before proceeding with a review of the studies that pertain most directly to the subject of this research, Fe_3Al, some of the most important dynamic mechanisms will be discussed:

a) In the "displacement model" a lattice atom was removed from its lattice site by a secondary collision with the resulting formation of a Frenkel defect. An alternate

mode of damage, the "replacement collision," was first postulated by Kinchin and Pease (10). They proposed that the moving atom might impart sufficient kinetic energy to the stationary atom for it to escape its lattice site; but, in so doing lose enough energy to become trapped in the potential well of the vacancy. This process might be called a "dynamic interstitialcy exchange" (after Billington and Crawford (11)). Although this mechanism was unobserved in pure metals, it was significant to property changes in order-disorder alloys. Leibfreid (12)(13) recognized the possibility that there might be a series of replacement collisions along a given crystallographic direction (such as [100] direction in Fe_3Al). The final configuration might be a vacancy and an interstitial separated by a long chain of replaced atoms. According to Leibfreid, this "replacement chain" would be expected to produce a large number of displacements detectable in a superlattice alloy such as Cu_3Au.

b) Brinkman (14) found that, for primary energies below 500 eV, collisions of heavy atoms may be considered using a hard sphere model, and the mean free path between collisions became comparable to, or even smaller than, the interatomic separation. If this was the case, then individual displacements would have little significance and the end of the path of the primary atom would be marked by the formation of a relatively large volume of disturbed material

($\sim 10^3$ atoms). Brinkman predicted that this region should contain a large number of Frenkel pairs, regions of mismatch, and dislocation loops. The "displacement spike" was very different from the "thermal spike" (below) since the primary was conceived of as a projectile plowing through the lattice, disturbing or churning up atoms along its path; although, in the end, the two spikes reduced to the same type of phenomenon. The only evidence remaining after a thermal spike should be the products of the reactions that occurred during the passage of the spike; while, the "displacement spike" would be associated with the formation of point defects, dislocations, mismatched regions, and more drastic disordering.

c) Seitz (15) noted the similarity between the lattice vibrations associated with the passage of a knock-on and those due to thermal effects. According to Seitz, the dissipation of a large amount of energy as the dynamic event slowed down caused the volume of the crystal immediately surrounding the dynamic event, called the "thermal spike" region, to behave as though heated to temperatures in excess of $1000^{\circ}K$ for a period of time on the order of 10^{-11} seconds. This local heating, followed by a subsequent rapid cooling, might help explain some of the disordering of superlattices, phase changes, and thermal generation of defects. The resulting change should approximate that found after heating to a high temperature and then rapidly quenching. After

further consideration, Seitz concluded that the amount of disordering in Cu_3Au expected from a thermal spike was insufficient to account for the experimental results. There was still good evidence, however, that phase changes might be enhanced by thermal spikes.

In the theories discussed above, the ordered arrangement of the atoms on a crystal lattice was almost completely neglected, and the basic treatment of displacements and spike phenomenon was a random arrangement of atoms resembling the real crystal in density alone.

d) In order to help explain the difference between the amount of disorder caused by the thermal spike model and that actually observed in Cu_3Au, Seitz and Koehler (16) introduced the concept of the "plasticity spike." They postulated that the expansion and deformation of the surrounding crystal during the sudden heating and cooling of the thermal spike might contribute to the disordering of Cu_3Au. Dislocation loops produced in the high temperature region would be available for deformation. Billington and Crawford, however, pointed out that the total disordering of Cu_3Au by strain in the absence of irradiation had not been observed; thus, the importance of this mechanism should be discounted.

e) Silsbee (17) was the first to consider the effect that crystal structure might have on radiation damage. The model that he proposed for this involved the transfer of energy or energy and matter along a close-packed row of

atoms in a series of "focusing collisions." This mode of damage might take on two basic forms. (1) If the energy of the initial knock-on, E, lay below some threshold energy, E_z, ($0<E<E_z$) then only energy would be transferred down the row, and this corresponded to the propagation of a "focuson." (2) If the energy, E, was greater than the threshold value, E_z, but less than some upper limit, E_f, ($E_z<E<E_f$), then both energy and mass were transported. The resulting defect, called the "dynamic crowdion," was physically very similar to the "replacement chain," as pointed out by Leibfreid, only in this case in a close packed direction. Since this mechanism died out rapidly, as the difference in atomic masses in a binary alloy increased, it was not expected to play a large role in disordering Cu_3Au.

The effect of nuclear bombardment on order-disorder reactions in alloys has received a great deal of attention. Order-disorder alloys are well suited to radiation damage studies since they often exhibit large physical property changes as the degree of order is altered. Cu_3Au, CuPt, and CuPd all show a marked resistivity decrease upon ordering, and the effect that irradiation has on order-disorder reactions may be inferred from these resistivity changes. There are numerous other properties that are sensitive to the degree of order. For example, the ordered state in Ni_3Mn (18) is strongly ferromagnetic, while the disordered state is not, and the Curie temperature of PtCo (19) alloys is

dependent on the degree of order. Magnetostriction, magnetic anisotropy, and coercive force are also known to be functions of the degree of order. The most important measure, however, of the degree of long range order is the presence of superlattice lines in X-ray diffraction patterns.

The first experiments on the effect of radiation on the order-disorder reactions were performed on Cu_3Au by Siegel (20), who observed that the electrical resistivity became progressively higher during neutron irradiation of the ordered alloy at room temperature while no resistivity change was observed for the disordered state, other than a slight increase due to transmutations. X-ray patterns later confirmed the decrease in order. Siegel found, using Seitz's method of defect calculation, that the amount of disordering introduced by irradiation was greater than expected by displacements alone, and it was necessary to employ the "thermal spike" concept to explain the results. This experiment might tend to confirm the thermal spike idea, but Kinchin and Pease (10) argued that the duration of the spike was not sufficiently long to produce the results seen, but a modification of Seitz's calculations, using the "replacement" concept, could adequately explain the results. Seitz and Koehler (16) concurred with Kinchin and Pease on the short duration of the spike and suggested, instead, that the thermal stress around a spike might be sufficient to cause

plastic flow in the immediate neighborhood, and that this might contribute to the disordering.

Kinchin and Pease were the first to consider the possibility of atomic replacements, and this model was later considered in detail by Dienes and Vineyard (21). They developed an analytical scheme to calculate the ratio of the number of replacement to the number of displacement events, given by

$$\frac{v_r}{v_d} = 1.614 \ln \frac{E_d}{E_r} + 1$$

where E_r was the energy needed to cause a replacement ($E_r < E_d$). A ratio of $E_d/E_r \approx 10$, considered reasonable by Kinchin and Pease, gave a ratio or replacements to displacements of 4.7, considerably less than a ratio of 10 to 1 first proposed by Siegel in 1949 yet sufficient to explain the rate of disordering in ordered Ni_3Mn and in the proper direction for disordering in the Cu_3Au system. It should be realized, however, that the above treatment was highly simplified since it assumed a monatomic solid; where, in reality, this process was of most importance for disordering of superlattice alloys. Any appreciable difference in mass would have an important influence on the displacement and replacement probabilities.

In the Cu_3Au system, first Siegel and then Brinkman, Dixon, and Meechan (22), using 9 MeV protons and 33 MeV alphas, indicated that the number of displaced atoms,

produced by irradiation, alone was not sufficient to cause the amount of disorder noted.

Of special interest was the discovery by D. E. Thomas (23) that radiation could both disorder an ordered alloy and order a disordered alloy thus increasing the complexity of the problem, since the rate of ordering or disordering now was a function of the degree of order already present. Ordering was attributed in Cu_3Au, by Walker (24), to (n, γ) recoils which were capable of imparting about 50eV to a gold atom which increased the probability of an ordering reaction. According to Pugh (25), the extent of ordering due to a given irradiation dose depended on the number of vacancies created and the average number of jumps before annihilation. In Cu_3Au, two types of ordering were found by Dugdale (26) to exist, each requiring a different number of jumps. The easy method involved the motion of the atoms to correct wrongly placed nearest neighbors, and the hard method involved correcting wrongly placed second nearest neighbors. Rudman (27) later noted that this effect could be explained by the homogeneity of vacancy concentrations, especially in the neighborhood of sinks where the concentration was found to be less. Experiments of Siegel (28), and Cook and Cushing (29) implied that approximately 10^4 atoms were rearranged per primary knock-on. Blewitt and Coltman (30) found that this number was too low by a factor of 100 to explain the amount of ordering seen in above room

temperature irradiation experiments on Cu_3Au, and could only justify the results by assuming that a large number of vacancies were present to cause the ordering. Brinkman, Dixon, and Meechan (31) have proposed that the vacancy was the defect causing ordering, since the number trapped increased as the quenching temperature for Cu_3Au was increased, and that the rate of ordering increased correspondingly. Since the copper atom could not easily displace a gold atom into an interstitial position, the migration of interstitials should not be responsible for ordering.

C. Radiation Effects on Fe_3Al

Betts (32) studied the effects of neutron irradiation on Fe_3Al and found, at constant temperatures, the resistivity of the ordered alloy would increase during irradiation, and the disordered alloy would decrease. Saenko (33) found the change in electrical properties occurred as though the long range order was being disrupted and the superlattice structure destroyed. The resistivity of the irradiated disordered alloy increased, which was evidence that some of the displaced atoms were returning to their lattice sites. The return of some superlattice lines in the X-ray diffraction patterns also confirmed these results.

Toma (34) investigated Fe_3Al and concluded that disordering increased by the production of displacement spikes and replacement collisions that disrupt the long range order. He also found that the vacancy-interstitial pairs and

interstitials produced by replacement collisions were metastable at elevated temperatures, since the degree of order increased as the temperature was lowered.

D. Computer Studies

In 1960, Gibson, Goland, Milgram, and Vineyard (35) proposed a method of investigating radiation damage that required no assumptions concerning what form the damaged configuration would take. This, also, provided evidence to support mechanisms that had been presented to explain radiation damage phenomenon and evidence to disprove others.

Previous attempts (36)(37)(38)(39)(40) to describe radiation damage events had required drastic approximations and it was generally assumed to consist of a sequence of independent two body collisions between the stationary and moving atoms, with the "knock-ons" moving freely between collisions. The atoms were treated as though randomly oriented and the only relation to the real material lay in a consistent density. The binding of the atoms to the lattice had been taken into account by assuming that the atoms would be displaced from their stationary positions if, and only if, endowed with a kinetic energy greater than some threshold energy, E_d, usually taken to be about 25 eV. By the cascade model, the damage configuration was assumed to be a complete set of a like number of interstitials and vacancies distributed randomly over a rather small region. Numerous other models, based on many body interactions, have been developed

out of the necessity of explaining experimental results that were inconsistent with a simple vacancy-interstitial cascade model. The thermal, displacement, and plasticity spikes, discussed previously, were of this nature. These models vary so much in detail that they were difficult to relate with one another, and to date no adequate explanation has been presented to resolve these differences. It was on this basis that Gibson et al. (35) concluded that a numerical approach might prove more informative than the previous analytical approaches had been.

Such a scheme involved considering a crystallite composed of a rather large set of atoms (500 to 1000) interacting with central two-body forces, with the stability of the lattice maintained by supplying additional forces to the surface atoms to simulate the binding effect of the crystallite being inbedded in an infinitely large crystalline matrix. The dynamic event was initiated with all but one of the atoms at rest on their normal lattice sites. The one moving atom corresponded to the primary knock-on, with some arbitrary velocity and direction as though just struck by some bombarding particle (such as a neutron). A high speed computer then integrated the motion of the primary knock-on and the other atoms with which it interacted, indicating changes in energies and positions of the atoms as they collided until, eventually, as the kinetic energy died away a stable configuration was formed.

Investigation of the energy and directional dependence of the damage process were investigated by making a series of "runs" with a wide variety of initial conditions. By estimating the initial positions of the atoms and then following the motion of these as the crystal relaxed, it was possible to determine the stability of various defects.

No further details of the program or method of calculation will be given here since the program of Gibson et al. was very similar to the one used in this study and the details may be found in the following section on experimental procedure.

The first program of this type was designed to represent the F.C.C. lattice of copper. Numerous "runs" were made with a wide variety of initial conditions representing both static and dynamic events. For the "static" calculations the positions of the atoms in the defect were estimated and the atoms in the computer generated crystallite were given these coordinates. Starting from rest the motion of the atoms was followed until a stable, or equilibrium, configuration was reached. Artificial damping techniques which set the kinetic energy equal to zero whenever it reached a maximum were often employed to speed the attainment of equilibrium. In some cases, it was necessary to impart a slight initial motion to some of the atoms to spoil the perfect symmetry of the arrangement and avoid "dead center" positioning, which had lead to false equilibria.

The results of the static calculations indicated that the vacancy was a normal defect and the near neighbors relaxed inward about 2.5% of the equilibrium distance ($\sqrt{2}$ in terms of unit cell length of 2.0) to help fill the void created by the vacancy; while, second nearest neighbors, and even some more distant atoms, relaxed outward about 1/20 as far as the near neighbors inward relaxation. The interstitial was also investigated thoroughly and found not to reside in the center of the unit cell cube but, rather, in a "split interstitial" configuration in which it shared a lattice site with another atom, the axis of the pair lying along a cubic axis with a separation of about 1.2 (again, where the lattice constant in the same units was 2.0). This configuration was originally postulated by Huntington and Seitz (38)(41), but, its stability was not established until this numerical approach was developed.

It was also possible to check the stability of two versions of the "dynamic crowdion" referred to as the "site centered" and "space centered" models (42). In no case was the crowdion found to be stable, but the rate of decay of this defect was so slow as to indicate a fairly "flat" potential in the neighborhood of the defect; and, it was felt that a slight change in interatomic potential might make it stable.

The results of the "dynamic runs" are, by the nature of the events studied, much more complex than the static results; so, to simplify this review only the major conclusions drawn

by Gibson et al. will be presented here.

The result of irradiation at low energies was found to consist of interstitials and vacancies, in confirmation of what had been earlier concluded. Thresholds for permanent atom displacement of 25 eV in the [100] and [110] directions and 85 eV in the [111] direction indicated the strong influence that direction and crystalline structure had on the dynamic events.

Even more interesting was the presence of "collision chains" propagating in the [110] and [100] directions with especially low energy loss in the [110] direction, as was anticipated by Silsbee (17). Focusing was prominent below the surprisingly low thresholds of 30 eV in the [110] and 40 eV in the [100] directions, and chains with energies of 25 or 30 eV were found to transport matter and energy in the manner of a "dynamic crowdion" producing an interstitial at the end of the chain. The dynamic studies also added justification to the idea that more replacements were produced than displacements, as was anticipated from the studies on order-disorder alloys by Silsbee (28).

Shortly after this study was completed, Erginsoy, Vineyard, and Englert (43) introduced a second, modified version of the Gibson et al. program, representing the B.C.C. alpha iron lattice. It was felt more insight could be gained by studying a representative sample of a different crystal structure. In general, the results of both the "static" and

"dynamic" calculations confirmed what had been concluded from the F.C.C. copper program. The vacancy was, again, found to be stable with near neighbors relaxing inward about 6% of the $\sqrt{3}$ equilibrium near neighbor separation and the second nearest neighbors relaxing slightly outward. As in the case of the F.C.C. lattice, a "split" configuration was the stable state for the interstitial atom; however, the orientation in the B.C.C. lattice was along the [110] axis, while that in the F.C.C. lattice was along the [100] axis.

The complete series of "runs," made to test the stability of various forms of the Frenkel defect indicated in all cases that close pairs were unstable against recombination and the minimum separation for the stability of a pair was particularly large in the [111] close-packed direction. Second neighbors were also unstable against recombination and the same strong orientational dependence of the minimum "stable pair" separation was found in both the F.C.C. and B.C.C. models.

The results of the "dynamic" runs were closely parallel to those obtained for copper in that the defect state was composed primarily of Frenkel pairs and interstitials, and the mode of damage was strongly dependent on the crystal structure. The "key" mechanism for displacement at low energies was the "replacement" collision by a knock-on, where the knock-on itself never went into an interstitial position but replaced one of its neighbors. Whether this was a first,

second, or third nearest neighbor depended on the initial direction of the knock-on. The "collision chain," probably the most important mechanism for separating the interstitial and vacancy, was found to be prominent at threshold energies in the [111] and [100] directions and at higher energies, about 100 eV, in the [110] direction.

Again, the threshold energy for permanent atomic displacement was strongly directionally dependent. The easiest direction for permanent displacement was near [100] at an energy of about 17 eV. Threshold energies of 34 and 38 eV were needed for the [110] and [111] directions respectively, with the direction dependence based on the position and extent of the potential barriers formed by the neighboring atoms. Actually, the lowest thresholds for the above mentioned directions occurred at a few degrees off the axis, where the threshold was limited by replacements outside the sphere of third neighbors.

Vineyard (44) made a third modification of the basic program to incorporate the order-disorder concept into a lattice representing Cu_3Au. Unfortunately, only a few runs were made with this program, but the results reported indicated that extensive disordering was found under all conditions.

Rudman (45) indicated the need for more computer studies, especially on order-disorder alloys. It was the purpose of this present thesis to attempt to add to the knowledge obtained through the use of computer programming by studying the B.C.C. ordered alloy, Fe_3Al.

Chapter III

EXPERIMENTAL PROCEDURE

A. Model

The model employed in these calculations was designed to represent the completely ordered state of the Fe_3Al alloy. The computer program (Appendix A) generated a 12x12x12 lattice (unit length was equal to one fourth the unit cell edge) composed of 559 atoms interacting with central two-body forces. An additional constant force was applied to the atoms on the surface of the crystallite to insure a stable B.C.C. configuration with the proper lattice spacing. For static equilibrium the constant force was chosen to just balance the attraction of the first and second near neighbors below the surface. Vineyard (42) pointed out that this force gives an increment of the total binding energy proportional to the increment of volume for small displacements of the surface atoms. The force could represent any binding energy that was a function of the volume and varied at the right rate to balance the Morse potential attractions. The conduction electrons in a monovalent metal represented this form of binding and, thus, the constant surface force, to the first approximation, represented the cohesive effect of the

conduction electrons.

Since the model crystal was a rectangular parallelopiped, the force was normal to face for atoms located in the face, normal to the edge (along the [110] direction) for edge atoms and directed along the cube diagonal toward atoms on the corners. It should be noted that this was not purely a central-force model, so that the Cauchy relations did not have to be applied to the elastic constants. It was found in the early runs that a very small initial error in the value of the constant force would lead to significant surface atom migration as the program proceeded and it was necessary to adjust the force constants through a variable parameter (RVT) until the constants were determined to sufficient accuracy.

The crystallite was considered to be embedded in a crystal of infinite extent. To apply this to the program it was necessary to supply additional spring forces to the surface atoms proportional to their displacement from their normal lattice positions to simulate the reaction of the surrounding continium to small displacements of the surface atoms. Because of the nature of the B.C.C. structure, additional spring forces were needed for the layer of atoms just below the surface. These were taken, more or less arbitrarily, to be about one two-hundredth as large as the spring constant for the surface atoms. Both the spring constant and constant surface force were calculated after the lead of Gibson et al.

(35) and a more complete description of the calculations will be found in Appendix B. In order to dissipate energy from the crystallite and thus aid the system to attain an equilibrium configuration, Gibson et al. and Erginsoy et al. (43) added a viscous force to the surface atoms which was proportional to the negative of their velocity. Vineyard (46) suggested that if the computer program were not run for an excessive length of time it would not be necessary to supply the viscous force, since no appreciable effect would be observed during short runs. Therefore, the viscous force was not employed in this program. The reasonable reaction of the surface atoms when unintentionally involved in a dynamic event tended to justify the approximate validity of the treatment given the surface atoms.

B. The Interaction Potential

At the present time there is a great deal that is not known about atomic interactions. Some information was available describing the interaction potential of atoms at very close approaches, through particle bombardment experiments, and at relatively large separations, but little is known about the form that the potential must take at intermediate separations where the bulk of the calculations for this program must lie. Therefore, whatever potential is selected can, at best, be only an approximation.

In order to incorporate as much realism in the potential as possible a combination of three potentials was

employed with each potential applying over the range of separations for which it appeared most suited (see Figures 3 and 4). Girifalco and Weizer (47) have stated that if any central, pairwise, interaction potential function were to adequately describe the atomic interactions in a stable crystal, it must satisfy the following conditions:

a) $\phi(r)$ must possess a minimum at some point $r=r_0$,

b) $\phi(r)$ must decrease more rapidly with r than r^{-3}, and

c) all elastic constants derived from $\phi(r)$ must be positive.

The Morse potential function satisfied the above conditions and was employed by Girifalco and Weizer with considerable success to describe a number of cubic metals in terms of their elastic constants.

Leamy (48) used the Morse potential to determine a heuristic model to explain the order dependence of the elastic coefficients in the iron-aluminum system. In his model, the constants for the Morse potential were determined from the equations for the elastic moduli in terms of an interaction potential, with the values of the elastic constants obtained experimentally. The Morse potential, with the constants determined by Leamy for Fe_3Al, was used in this program to describe the atomic interactions at relatively large separations, $r > 1.30$. The near neighbor separation (in the same units) under equilibrium conditions is $\sqrt{3}$ and thus lies in the range of the Morse potential.

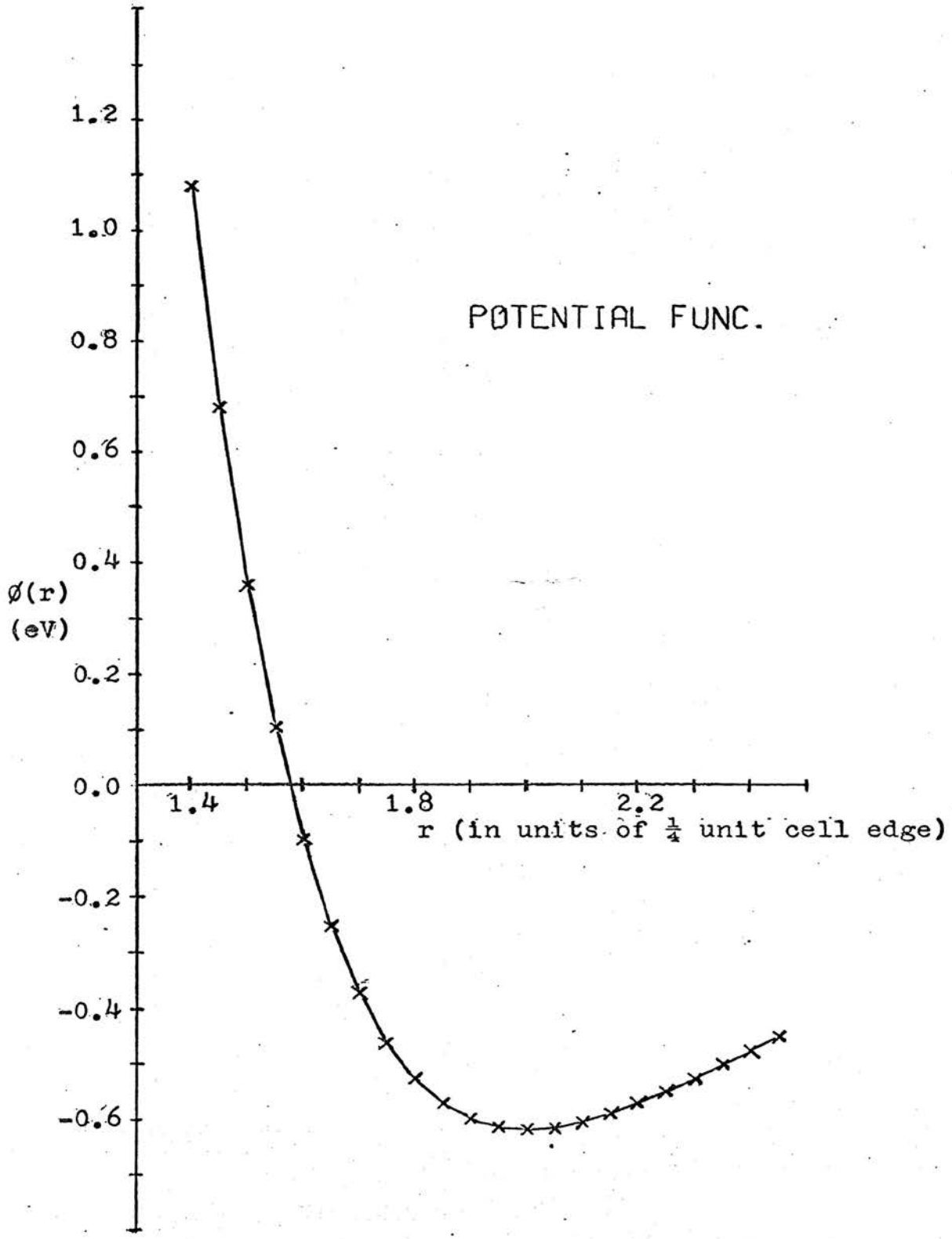

Figure 3 Potential Function for Equilibrium Separations

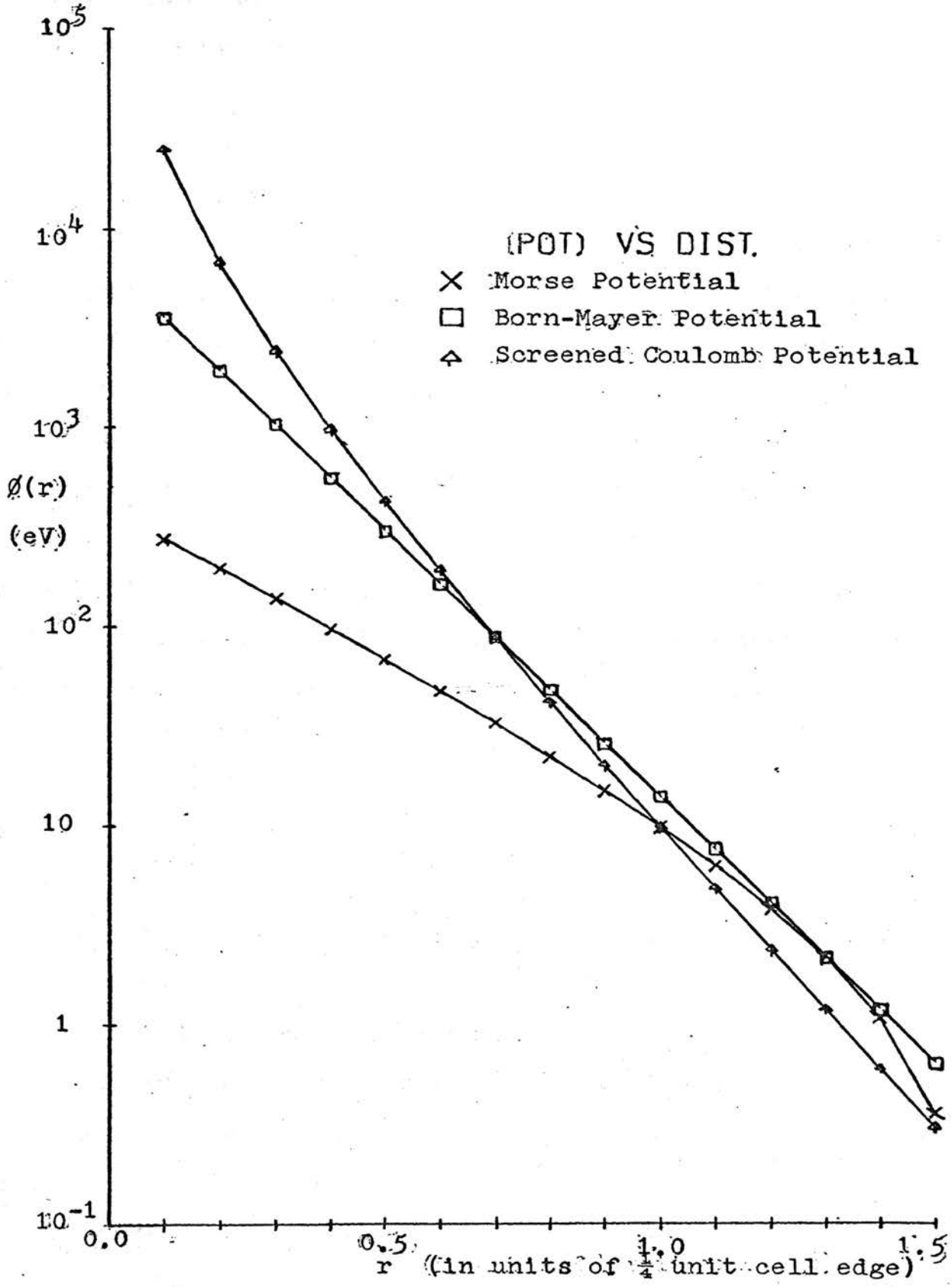

Figure 4 Three Potentials for Determining Atomic Interactions

The Morse function employed is given by the equation:

$$\phi(r) = D\left\{\exp\left[-2\alpha(r-r_o)\right] - 2\exp\left[-\alpha(r-r_o)\right]\right\} \qquad (1)$$

where:

$D = 0.6205$ eV $\qquad r_o = 2.0000$ units

$\alpha = 1.6280$ units^{-1}

Since the crystallite was stable with only second nearest neighbor interactions considered, the Morse potential was cut off at an interatomic distance of 2.5. It should be mentioned that this same potential was used in the calculation of the constant surface forces (see Appendix B).

For the intermediate separations, $0.7<r<1.3$, a Born-Mayer potential, chosen originally after the work of Huntington and Seitz (41) on point defects, was employed. The constants for this function were obtained by equating its value and slope to that of the Morse potential at a separation of $r=1.3$, with the resulting equation:

$$\phi(r) = A\ \exp(-Br) \qquad (2)$$

with,

$A = 6550$ and $B = 6.1500$

For the closest approaches, $r<0.7$, a screened Coulomb potential was deemed most reliable, and this function was extrapolated directly from the Born-Mayer potential at a separation of $r=0.7$. The Coulomb potential is:

$$\phi(r) = (0.7/r)\ A\ \exp(-Br) \qquad (3)$$

with,

$A = 6550$ and $B = 6.1500$

The Morse function was considered the most accurate of the three and, therefore, no attempt was made to investigate the effect of altering the constants in the function on the experimental results. The constants in the Born-Mayer potential were changed by matching the function with the Morse potential at a separation of r=1.35. The change had little effect on the threshold energy in the [100] direction and no further changes were attempted. It should be noted that this combination of three potentials was first used by Erginsoy, et al. (43) in work, described previously, on B.C.C. alpha-iron.

C. Calculations

Solving a complete series of exact differential equations describing the motion of the entire set of atoms would require a substantial amount of computer time. This method of calculation inherently exhibits more accuracy than was necessary, especially in light of the approximate nature of the interaction potential. It was decided that a central difference scheme would be more efficient, as it would allow for sufficient accuracy with reasonable speed.

Let the ith atomic coordinate be designated at any time, t, by $x_i(t)$ and the associated velocity by $v_i(t)$ where i=1, . . ., N is three times the number of atoms in the crystallite. The force on the ith degree of freedom will be a function of the position of all of the atoms, and the force

may thus be written as:

$$F_i(x_1(t),....,x_N(t)). \qquad (4)$$

If m is the mass of the particle under consideration, then the classical equations of motion become (dots represent derivatives with respect to time):

$$\dot{v}_i(t) = m^{-1} F_i(x_1(t),...., x_N(t)) \qquad (5)$$

$$\dot{x}_i(t) = v_i(t) \qquad i=1,2,...,N \qquad (6)$$

In applying the central difference scheme we replace the time derivatives by finite differences with some arbitrary time interval Δt (see Appendix C for units used in calculations) and calculate new coordinates at each integer step and new velocities at each half integer step.

Thus:

$$\dot{v}_i(t) = (v_i(t+\Delta t/2)-v_i(t-\Delta t/2))/\Delta t \qquad (7)$$

$$\dot{x}_i(t+\Delta t/2)=(x_i(t+\Delta t)-x_i(t))/\Delta t \qquad (8)$$

By manipulation of the above equations, we obtain those used in the computer programs:

$$v_i(t+\Delta t/2)=v_i(t-\Delta t/2) + \Delta t\, m^{-1}F_i(x_1(t),..,x_N(t)) \qquad (9)$$

$$x_i(t+\Delta t)=x_i(t)+\Delta t\left(v_i(t+\Delta t/2)\right) \qquad i=1,2,...,N \qquad (10)$$

Starting at any arbitrary time (t) with a complete set of positions, $x_i(t)$'s, and velocities, $v_i(t-\Delta t/2)$'s, the machine iterates on these to calculate a new set of coordinates $x_i(t+\Delta t)$ and velocities $v_i(t+\Delta t/2)$. This new data is then used to calculate positions and velocities of the atoms

at time, $t+2\Delta t$, and this process is repeated successively for $t+3\Delta t$, $t+4\Delta t$, etc.

The optimum choice for the size of Δt depended on the maximum velocity of the most energetic atom. If the chosen Δt was too small, the program would require excessive computer time; while if the time step was too large, a significant error would be introduced into the calculations through the approximate nature of the central difference scheme.

The choice of Δt had been studied closely by Gibson, et al. (35), with the same program run with a variety of time increments. Good results were obtained for maximum velocities corresponding to an energy of about 25 eV and $\Delta t=1$; for energies of 100 eV, $\Delta t=1/2$. At higher energies, about 400 eV, $\Delta t=1/4$. Since the present study involved, predominently, energies in the range 30 eV to 60 eV, $\Delta t=1/2$ was employed for all the early stages of the dynamic events.

As the energies of the atoms were decreased through interactions, the time step was increased to speed the formation of a stable end configuration. For some longer runs $\Delta t=1/2$ was used for the first 60 to 70 time units and then increased to $\Delta t=1$ for the next 10 to 20 time units to insure the presence of an equilibrium state.

The central difference technique lead directly to a strict energy conservation law, analagous to the energy conservation laws of classical mechanics. This case could be seen by noting that the equations:

$$v_i(t+\Delta t/2) + v_i(t-\Delta t/2) = \Delta t^{-1}(x_i(t+\Delta t) - x_i(t-\Delta t)) \quad (11)$$

and

$$m(v_i(t+\Delta t/2) - v_i(t-\Delta t/2)) = \Delta t F_i(x_1(t)\ldots,x_N(t-\Delta t)) \quad (12)$$

were multiplied together to give:

$$(m/2)(v_i^2(t+\Delta t/2) - v_i^2(t-\Delta t/2)^2) = F_i(x_1(t)\ldots,x_N(t))* \\ 1/2(x_i(t+\Delta t) - x_i(t-\Delta t)) \quad (13)$$

which demonstrated that the increase in kinetic energy, for the ith degree of freedom in any one time step, was equal to the effective work done during that same time step. Equation 13 was written for each time step and summed over all the time steps from t=0 to t=T, where T was the total time of the program run. From this, the master conservation law could be implied:

$$K(T) - K(0) = -(\emptyset(T) - \emptyset(0)), \quad \emptyset(T) = \emptyset(X(T), Y(T), Z(T)) \quad (14)$$

where K(T) was the total kinetic energy of the system at time, T, given by:

$$K(T) = (m/2)\sum_{i=1}^{N} v_i^2(T+\Delta t/2). \quad (15)$$

$\emptyset(0) - \emptyset(T)$ was the sum of the work done by all the conservative forces in terms of finite differences, and was essentially a form of pseudopotential. If M was the total number of time steps such that, $M\Delta t = T$, then:

$$\emptyset(T) - \emptyset(0) = -\sum_{i=1}^{N} \sum_{t=1}^{M} F_i(x_1(M\Delta t),\ldots,x_N(M\Delta t)) * \\ x_i(M\Delta t + \Delta t) - x_i(M\Delta t - \Delta t) \ /2 \quad (16)$$

with $\emptyset(0)=0$ initially. In the limit, as $\Delta t \to 0$, the summa-

tion approaches a Riemann integral and $\phi(T)$ approaches the classical potential energy function $v(r)$.

The kinetic energy was calculated at each time step and used in equation 16 to calculate the pseudopotential $\phi(r)$. The classical potential $v(r)$ was also computed at the same time step from its analytical form and compared with the values of ϕ. If the difference in the two values was greater than some preset tolerance, the computer repeated the same calculation. If the difference was still too large, the program was exited and an error message was printed. If the difference was less than the tolerance, the machine proceeded to the next time step. Although the value of the discrepancy rarely exceeded a value of 1 in these calculations, the tolerance was normally set at 10 to allow for the possibility where speed of convergence was more important than great accuracy.

In order to solve for the force exerted on the ith particle, it was necessary to know the position coordinates of all the other particles with which this particle might interact. This could be accomplished for each particle by scanning all the other particles for interactions, and the time for this could be cut in half by saving the interaction force of i on j for when the force of j on i was needed. Even at this rate, the time for the search process would increase as the square of the number of particles.

A. Larsen (49), who did the computer programming for

Gibson, et al., reported the use of a "search box" technique that reduced the search time to a linear function of the size of the crystallite. This same scheme was employed in this program.

In the "search box" method, the crystallite was divided into boxes one fourth the unit cell length of Fe_3Al on each side with the limits of the volume described by these boxes as:

$$-.5 < X < IA + .5$$

$$-.5 < Y < IB + .5$$

$$-.5 < Z < IC + .5$$

where IA, IB, IC, were the crystallite dimensions in the X, Y, Z directions, respectively.

From the X, Y, and Z coordinates of the center of each box, an identification number was determined by:

$$J=(X+1.5+\alpha(Y+.5)+\beta(Z+.5)) \qquad (17)$$

with $\alpha = IA+2$ and $\beta = IB+2$. To determine the box in which a given particle was located, the coordinates of the particle are substituted into the equation for the box identification number. Box (J) was an array in which the particle number or numbers corresponding to a given box location were stored and in which a maximum of three particles could be located simultaneously. The only interactions which are considered important were those of the near neighbors, so only the interactions with particles in the same box and neighboring boxes were considered. Those neighboring boxes that might

contain near neighbors of a particle must satisfy the conditions that:

$$|X-X_N| < 3, \quad |Y-Y_N| < 3, \quad |Z-Z_N| < 3 \tag{18}$$

and

$$|X-X_N| + |Y-Y_N| + |Z-Z_N| < 6 \tag{19}$$

(to eliminate corner boxes from consideration). A table of movements was set up for each of the 27 possible atom locations and these increments determined the coordinates of the boxes to be searched. Obviously the table of increments for the surface particles was smaller than the corresponding table for an interior particle. The array IDUX contained the length of these tables and the array IAUX contained the subscript of the first entry in each table.

Chapter IV

EXPERIMENTAL RESULTS

Using the computer program previously described, a series of twenty-six dynamic events, representing a variety of knock-on directions and energies in a basic 12 x 12 x 12 B.C.C. Fe_3Al crystallite, have been investigated. In order to simplify the presentation of the results, only those events that were most representative will be discussed fully while a complete listing of the runs performed will be found in Appendix D. In all figures in this section depicting damage events, the large open circles represent atoms in the plane under consideration; while the smaller circles represent atoms in the plane immediately below. Both large and small circles that are "crossed" indicate aluminum atoms and the open circles indicate iron atoms.

A. Dynamic Events in [100] Direction

The first dynamic event originated in the [100] direction with an iron atom at position (6,6,6) endowed with an energy of 46 eV. The mechanics of this event soon extended beyond the boundary of the crystallite. Figure 5 depicts the same event initiated at an iron atom on position (2,6,6) at the far side of the crystal in an attempt to contain the

majority of the dynamic sequence. In Figure 5, the point A_1 marks the initial position of the knock-on with the motion of this and all other atoms in the two planes indicated by the solid lines originating at the circle centers.

As the 46 eV knock-on was displaced to the right along the [100] line of Fe atoms, its kinetic energy decreased. This decrease was initially relatively slow, but as the knock-on approached the potential barrier formed by the two body-centered atoms (P_1 and P_2) below the path of the knock-on and the two body-centered atoms above (not shown), the decrease was greatly accelerated. By the time the knock-on had reached the apparent saddle point of the barrier, B_1 (midway between A_1 and D_1), its kinetic energy was reduced to just below 30 eV. After passing the saddle point B_1, the kinetic energy continued to decrease very rapidly, due to the repulsion of the second atom in the chain at D_1 (4,6,6). By C_1 the knock-on was nearly stationary with an energy of .148 eV. Figure 5 shows that the knock-on replaced the second atom at D_1 and this atom, likewise, extended the "replacement chain" through positions E_1 (6,6,6) and F_1 (8, 6,6).

After 80 time steps, the program was terminated with an interstitial formed somewhat past F_1 and a vacancy remaining at A_1. The atoms forming the barrier planes, such as P_1 and P_2, expanded slightly away from the path of the knock-on as it passed and subsequently returned to their normal lattice

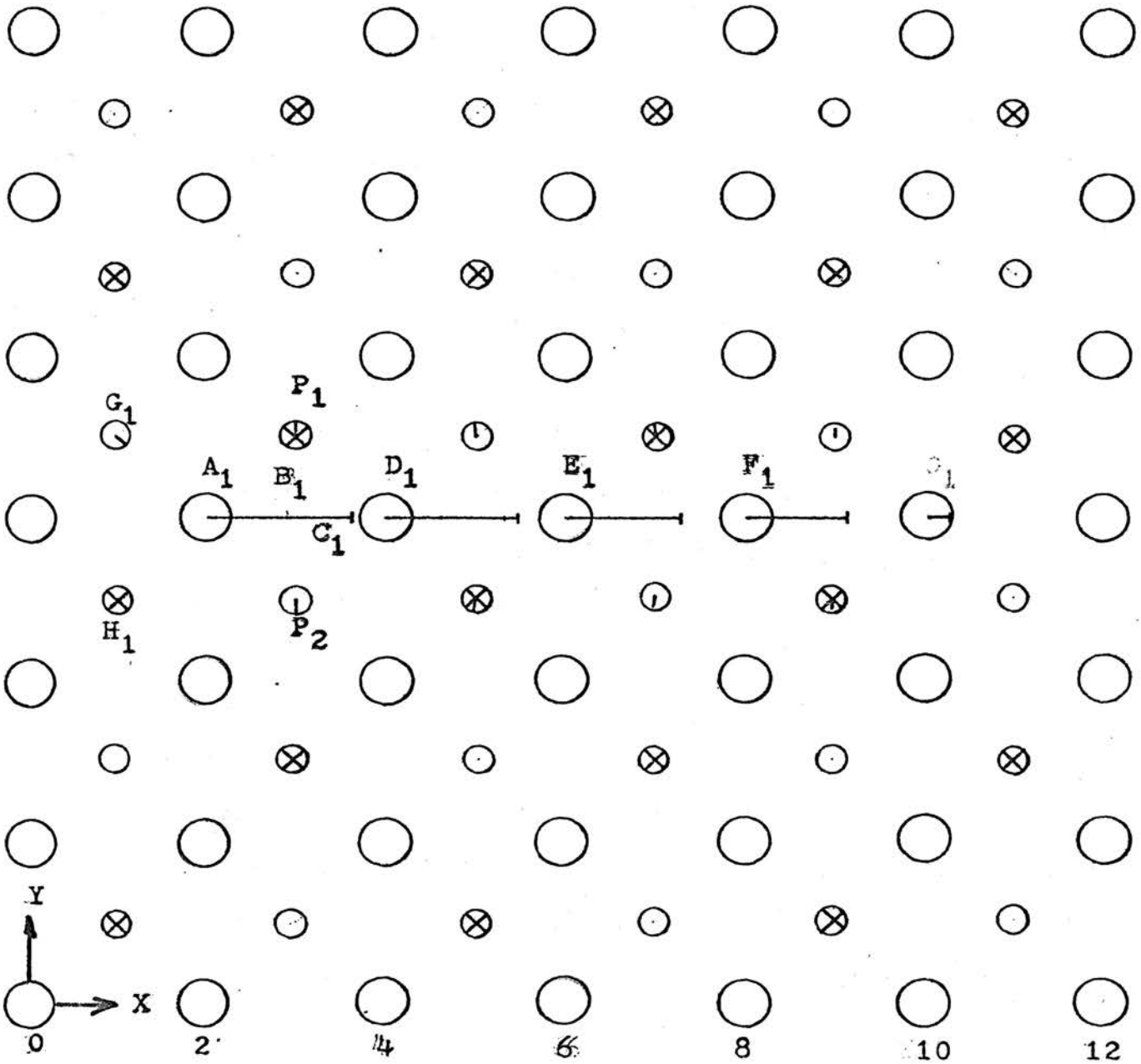

46eV Knock-on in the [100] Direction.
Figure 5

sites. The atoms at G_1 and H_1 relaxed slightly inward to fill the void created by the vacancy.

The relation of the positions of the atoms in the "collision chain" to the time, measured from the initiation of the knock-on event, may be seen in Figure 6. It should be noted that the distance of closest approach between the atoms in the chain was very nearly a constant with only a slight increase apparent as the "collision chain" progressed and the kinetic energy pulse died away.

Figure 7 (bottom) shows the change in the magnitude of the kinetic energy pulse for successive time steps. The initial kinetic energy drop between peaks K.O. and X_1 was about 11 eV, while the kinetic energy drop between X_1 and X_2 and all subsequent peaks was approximately 5 eV. The minima in Figure 7 corresponded to the minimum kinetic energy of the moving atom just past the equilibrium saddle point (B_1 in Figure 5). The minimum kinetic energy of the system remained fairly constant throughout the run as indicated by minima in Figure 7.

A series of runs were made with energies ranging from 20 to 50 eV in the [100] direction to determine the threshold level for permanent displacement. For a [100] chain of entirely iron atoms, such as the event described above, this threshold was found to be about 22 eV.

B. Focusing Collision in [100] Direction

Figure 8 depicts a 107 eV knock-on (at A_2) initiated with an iron atom at (2,6,6) 1.5° away from the [100] direction. The propagation of this knock-on was essentially the same as the 46.0 eV case described above with the eventual occurrence of replacement collisions at B_2 (4,6,6), C_2 (6,6,6), D_2 (8,6,6), E_2 (10,6,6), and F_2 (12,6,6). An interstitial formed past F_2 with a vacancy left at A_2. Note that the degree of defocusing increased as the chain progressed. Not shown in the figure was the tendency for the collision chain to defocus preferentially downward in the -Z direction, toward the aluminum atoms at P_1, P_4, etc. Notice in Figure 8 that the elevation of the path of atom B_2 at point T_1 is .0300 units below the plane of action, while at T_2 it is .0062 units above. The small motion of the atoms immediately surrounding the collision chain was very similar to that seen in the 46 eV case, Figure 5.

The curve at the top of Figure 7 indicated that an energy of about 13 eV was needed to initiate the defocusing events, while only about 4 eV was lost at each subsequent collision. Again the minima corresponded to the minimum kinetic energy associated with an atom when it was located at the equilibrium saddle point formed by the potential barriers at P_1, P_2, P_3, P_4, etc. The tailing off of the kinetic energy curve, top of Figure 7, and the less distinct maxima and minima near the end of the curve indicate the kinetic energy was being defocused away from the [100]

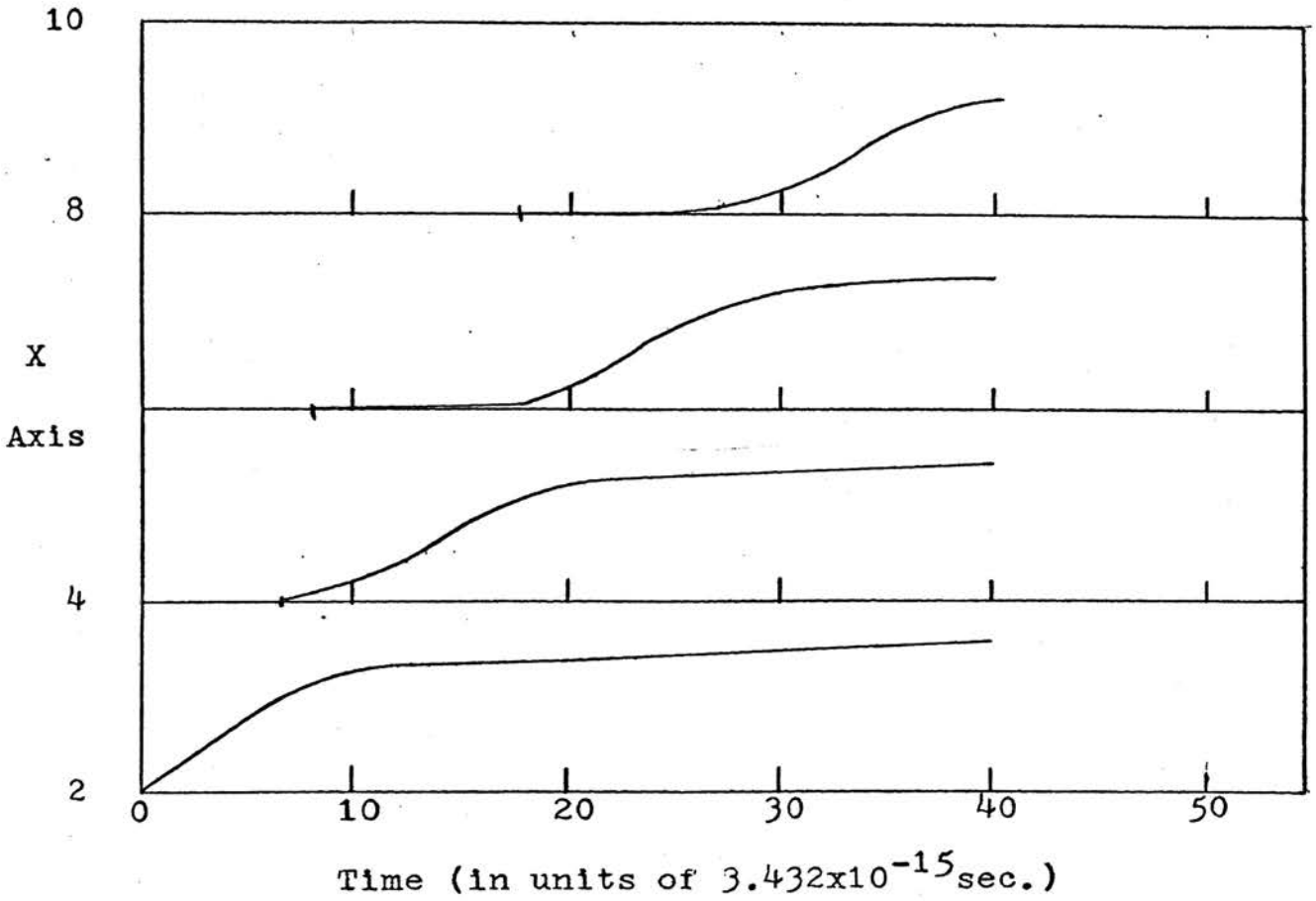

Figure 6 Replacement Chain in [100] Direction from 46eV Knock-on.

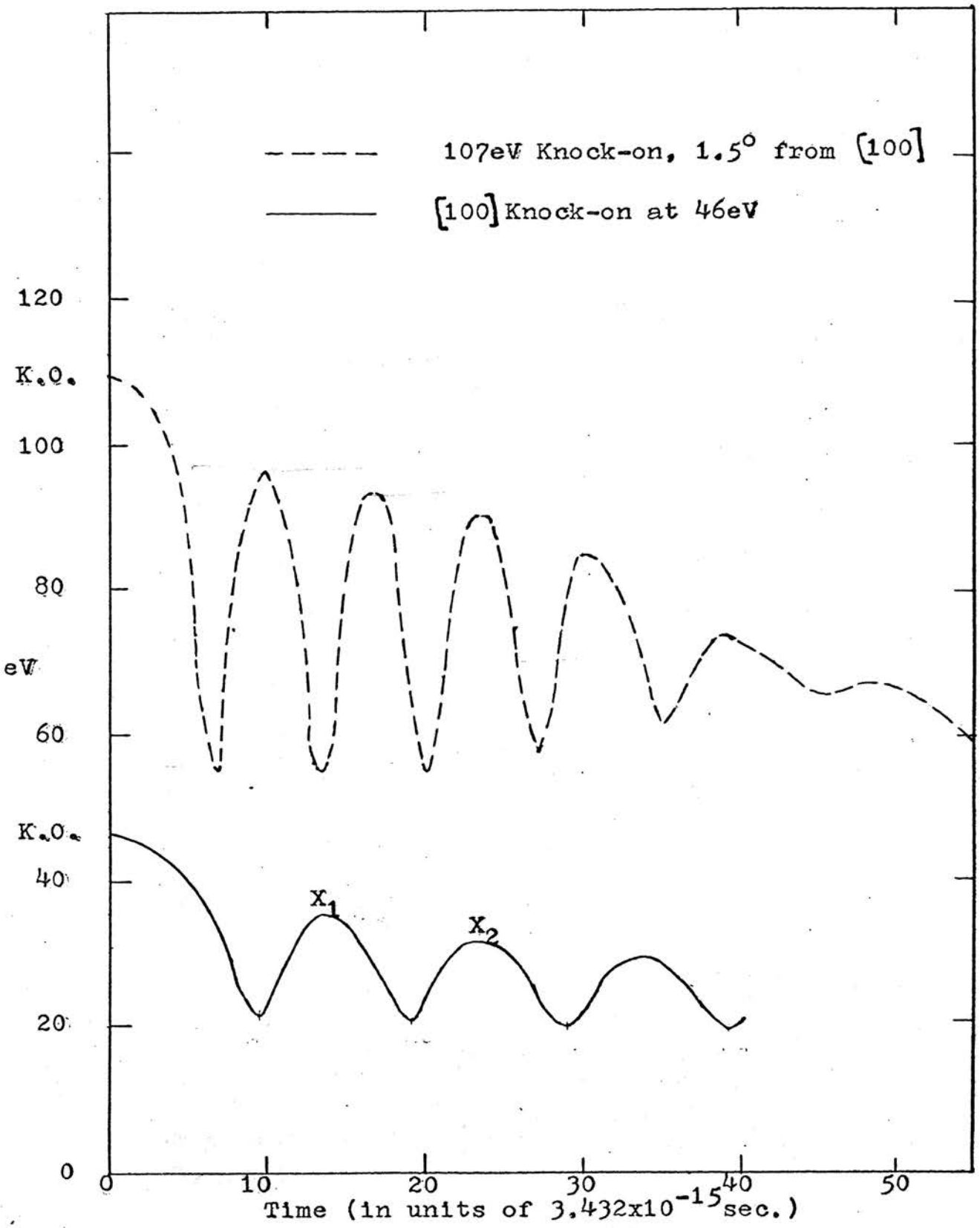

Attenuation of Kinetic Energy Pulse.

Figure 7

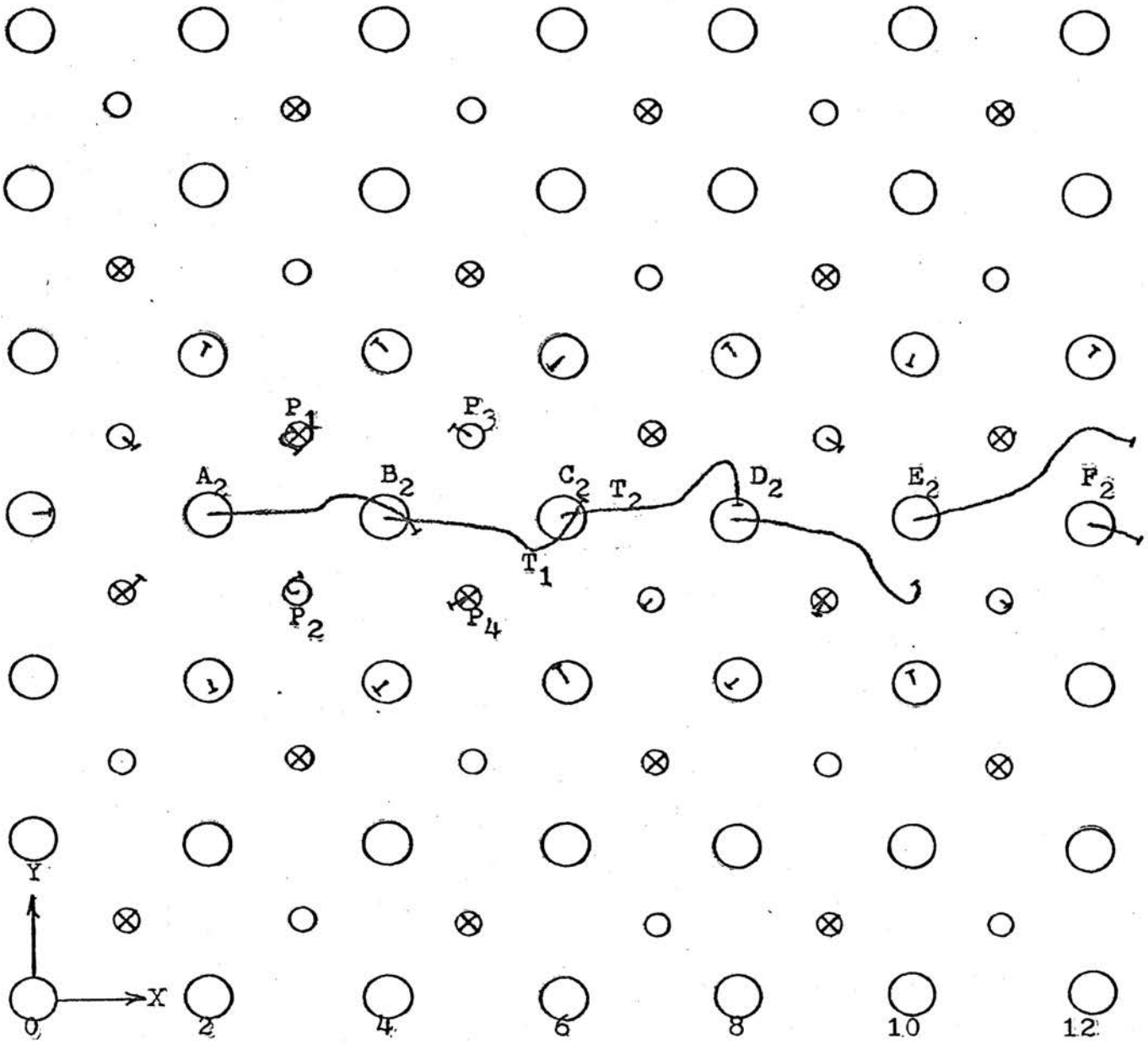

Defocusing in the [100] Direction at 107eV.
Figure 8

direction; thus, the effect of the potential barrier planes along the [100] direction was being reduced.

A second [100] focusing collision chain was tried with the same knock-on energy (107 eV) as the previously described run as shown in Figure 10. The location of the knock-on site was an aluminum atom at (3,7,5) instead of an iron atom at (2,6,6). The knock-on site was point A_5 in Figure 9. The aluminum knock-on, A_5, made one complete oscillation in its potential well during the 55 time steps. The iron atoms in the collision chain showed a simple defocusing motion, while the aluminum atoms exhibited more drastic behavior. Defocusing of the displaced atoms and energy was prominent along the chain with an especially large degree of defocusing occurring at the aluminum atom, C_5 (7,7,5).

A series of replacement collisions occurred along the [100] chain at the points C_5, D_5, and E_5. An interstitial would have occurred considerably past F_5 had the crystal been large enough to contain the entire event since at the point F_5 the kinetic energy pulse had only been reduced to a value of 69 eV from the knock-on energy of 107 eV. It should be noted also that from the time the displaced atom E_5 passed the point F_5 the kinetic energy pulse remained at or about a value of 69 eV.

The most significant point to consider in this trial was the formation of a vacancy at B_5 and not at the knock-on

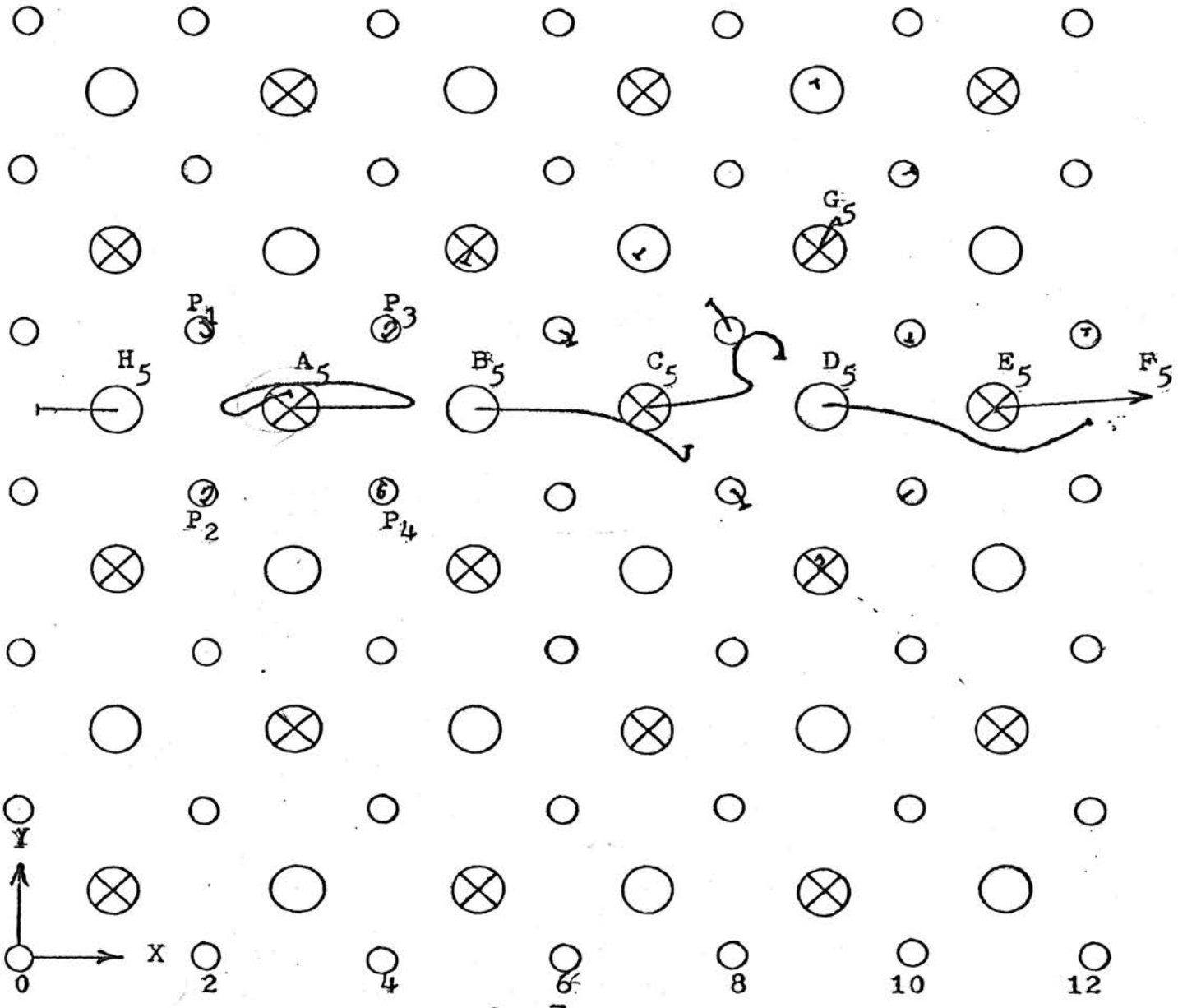

Defocusing in the [100] Direction at 107eV
Starting at an Aluminum Atom.
Figure 9

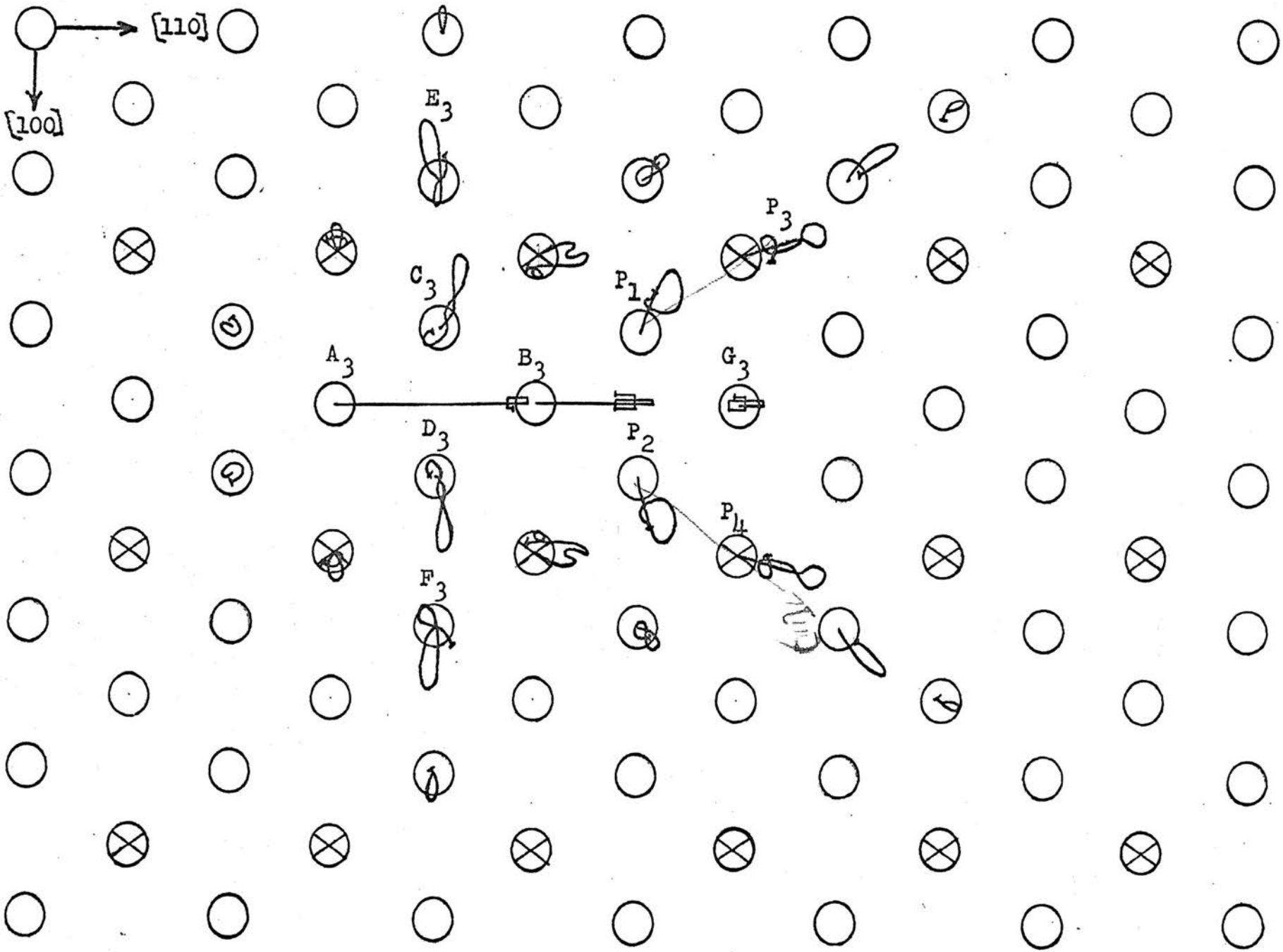

Figure 10 50 eV Fe Knock-on in the [110] Direction

site, A_5, as in the other replacement collisions studied.

Atom H_5 was displaced in the negative [100] direction because of the oscillation of the aluminum knock-on at A_5.

The surrounding atoms at P_1, P_2, P_3, P_4, etc. that formed the [100] potential barriers alternately dilated and contracted to allow the passage of the atoms in the collision chain.

C. Dynamic Events in the [110] Direction

A [110] collision chain is shown in Figure 10 initiated by an iron atom at position A_3, (3,3,7), with an energy of 50 eV. The knock-on replaces the iron atom B_3, at (5,5, 7).

A series of "focusons" in the [100] (at C_3, E_3, and D_3, F_3) and [111] (at P_1, P_3 and P_2, P_4) directions focused the majority of the energy of the kinetic energy pulse away from the [110] collision chain. This resulted in the displaced atom from B_3 not possessing sufficient energy to penetrate the potential barrier formed by atoms P_1 and P_2 and thus it was trapped in the same potential well as the original knock-on atom. The two atoms then formed a di-interstitial at B_3. The arrangement of this split-interstitial was similar to that observed by Erginsoy et al. (43) except that the center of gravity of the interstitial pair was located to the right of the location determined by Erginsoy.

Figure 11 shows the positions of the atoms in the 110

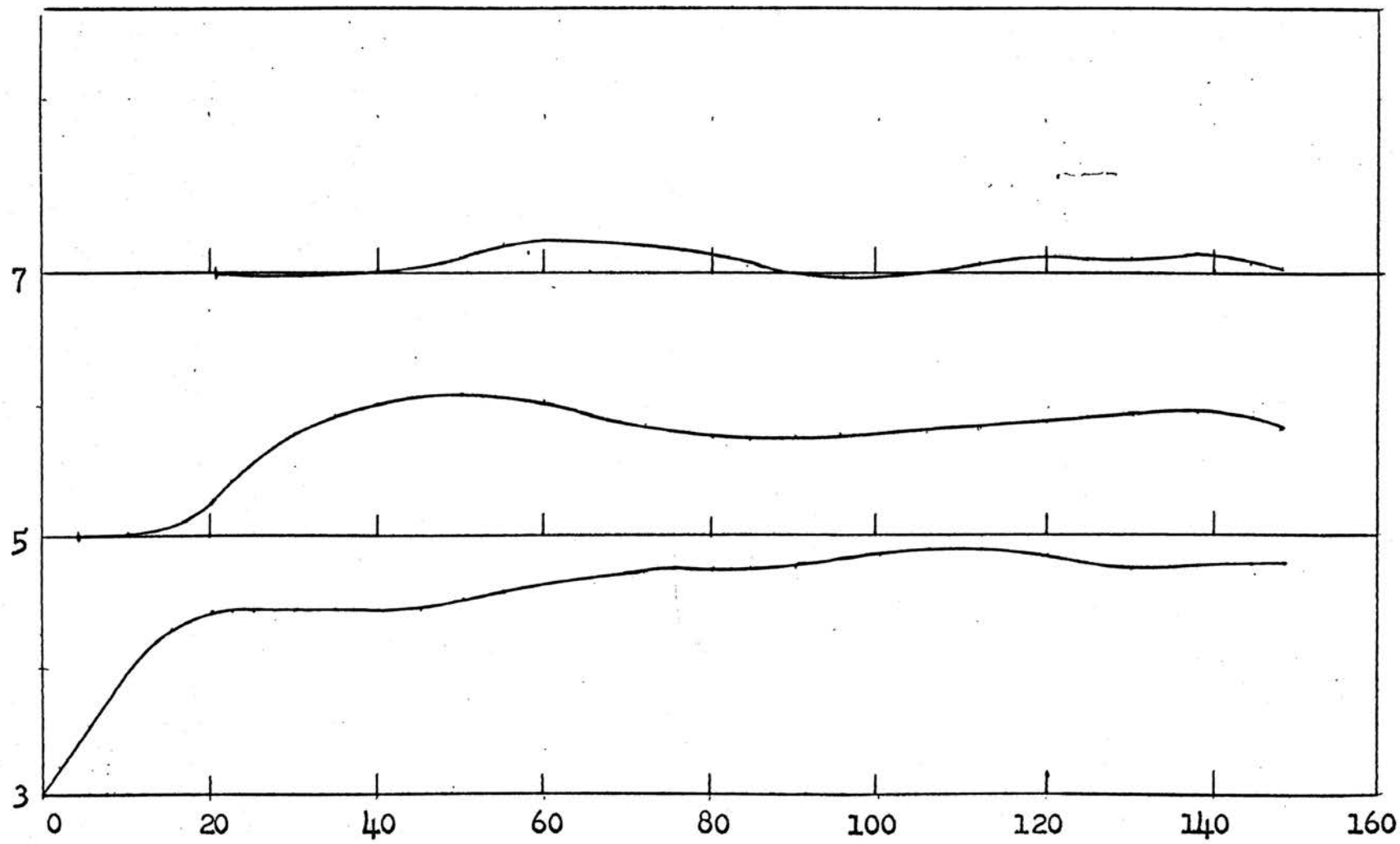

Figure 11 Replacement Chain in [110] Direction from 50 eV Knock-on

collision chain with respect to time. It should be noted that the atom originally located at G_3 (position X = 7 in Figure 11) was initially attracted to the interstitial atom B_3 (position X = 5) before being repelled and forced in the positive [110] direction.

As in the [100] study, a series of runs corresponding to a variety of primary knock-on energies was made to determine the threshold for permanent displacement of an iron atom in the [110] direction. The threshold for displacement of the iron atom located at (3,3,7) described above was found to be about 44 eV. Several additional runs were made in the [110] direction starting with an aluminum atom at location (3,3,5). The mechanics of the dynamic events, involving a chain of aluminum atoms, were essentially the same as for the all iron chain. Again, the threshold energy for permanent displacement of an aluminum atom was found to be about 44 eV.

D. Dynamic Events in the [111] Direction

The events described up to this time involved collision chains containing atoms of only one species, either all iron or all aluminum. As indicated in Figures 12, 13, 14, and 15, the mechanisms involved in the motion of the atoms in a [111] collision chain were much more complex. Figure 12 shows that the motion of the aluminum knock-on (50 eV) involved several oscillations of the aluminum atom through

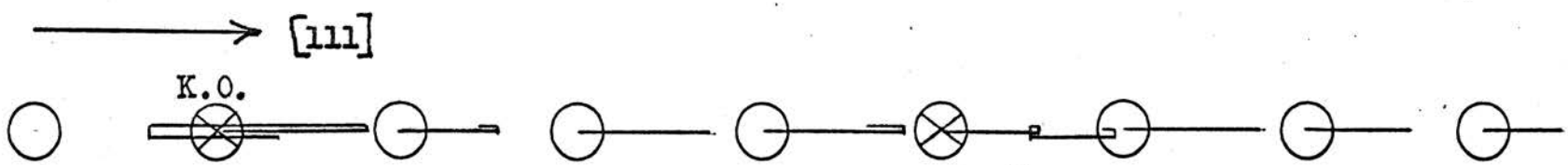

Figure 12 Collision Chain in the [111] Direction
Initiated with a 50.7 eV Aluminum Knock-on

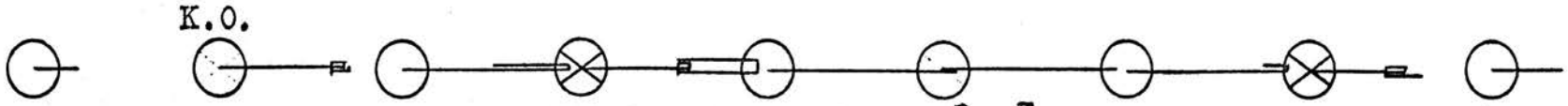

Figure 13 Collision Chain in the [111] Direction
Initiated with a 50 eV Iron Knock-on

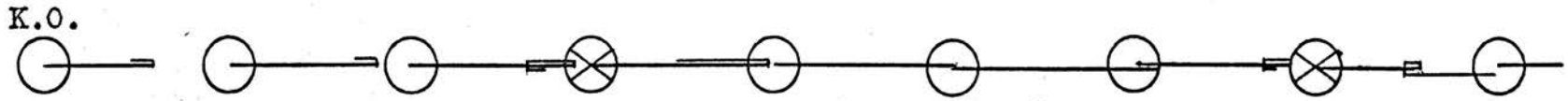

Figure 14 Collision Chain in the [111] Direction
Initiated with a 57 eV Iron Knock-on

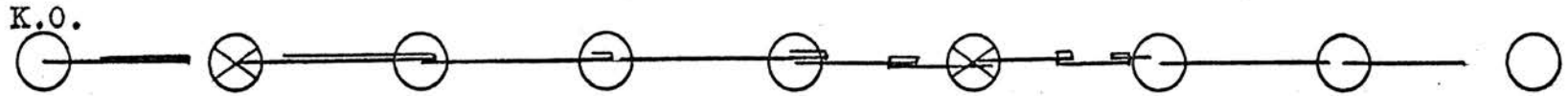

Figure 15 Collision Chain in the [111] Direction
Initiated with a 59 eV Iron Knock-on

its potential well with corresponding little motion of the iron atoms along the chain. In no case was an aluminum knock-on displaced permanently from its normal lattice position. Figures 12, 13, 14, and 15 show the marked effect that the position of the aluminum atoms, relative to the knock-on, has on the mechanics of the dynamic events. It may be seen in Figure 15 that the maximum motion of the atoms along the collision chain occurred when the knock-on was an iron atom followed in the collision chain by an aluminum atom.

Figures 16 and 17 show the relation of the positions of the atoms in the collision chain to the time for a 50 eV iron knock-on and a 50.7 eV aluminum knock-on, respectively. The motion of the iron atoms in both figures is very similar to the motion seen in Figures 6 and 11 for the [100] and [110] directions.

The only event, initiated in the [111] direction, to result in a permanent displacement of an atom was for a knock-on energy of 89 eV. In this case the displaced atom was not the knock-on, but, rather, an iron atom five atoms down the collision chain.

Figure 18 shows the attenuation, with time, of the kinetic energy pulse for the 89 eV and 50 eV runs. Unlike Figure 8, the curves do not show the steady decrease in the energy peaks and the relatively levelness of the minima. It should be noted, from the curves, that at an 89 eV knock-on energy, 16 eV was required to initiate the collision chain

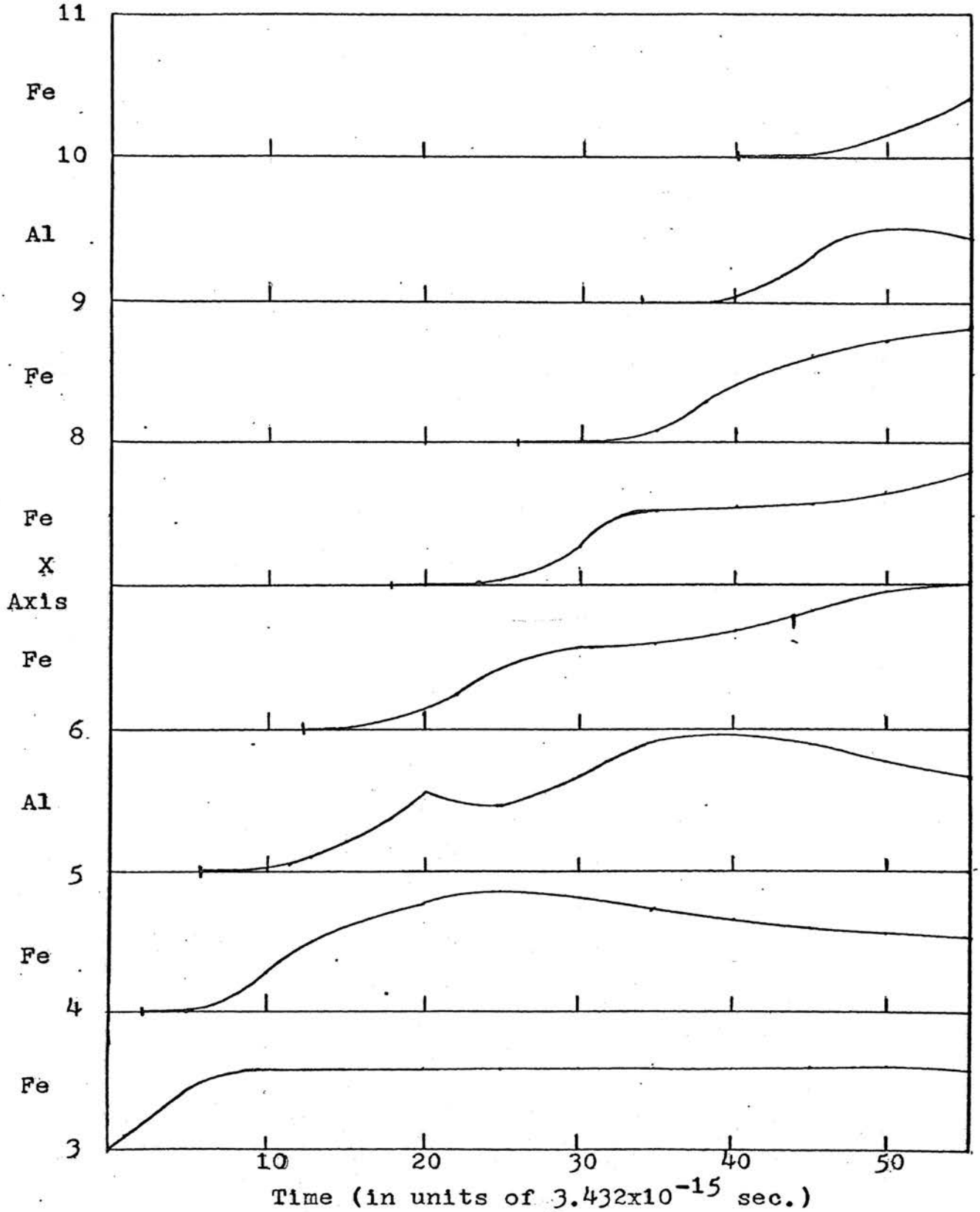

Figure 16 Replacement Chain in [111] Direction from 50.7eV Fe Knock-on

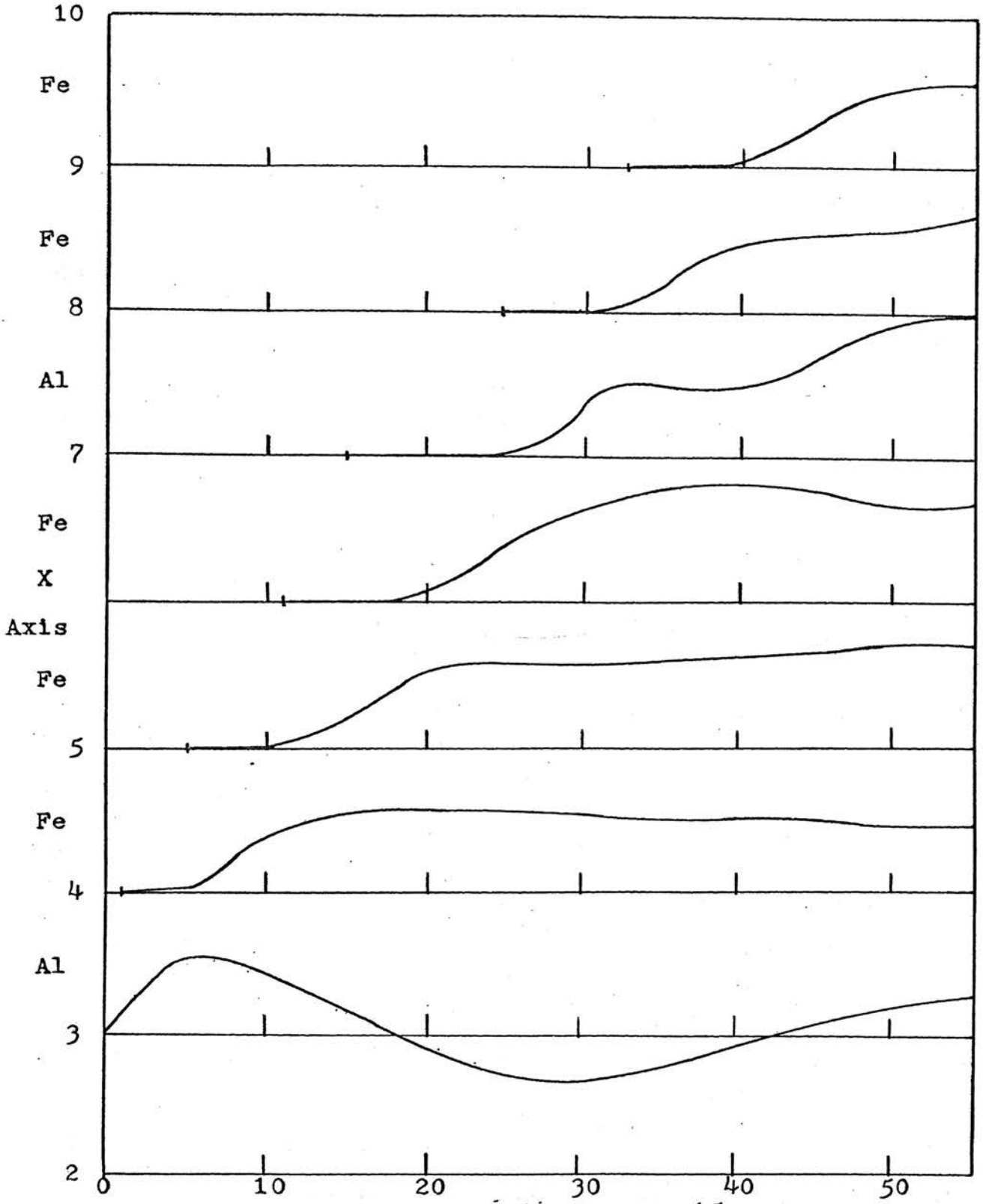

Figure 17 Replacement Chain in [111] Direction from 50.7 eV Al Knock-on

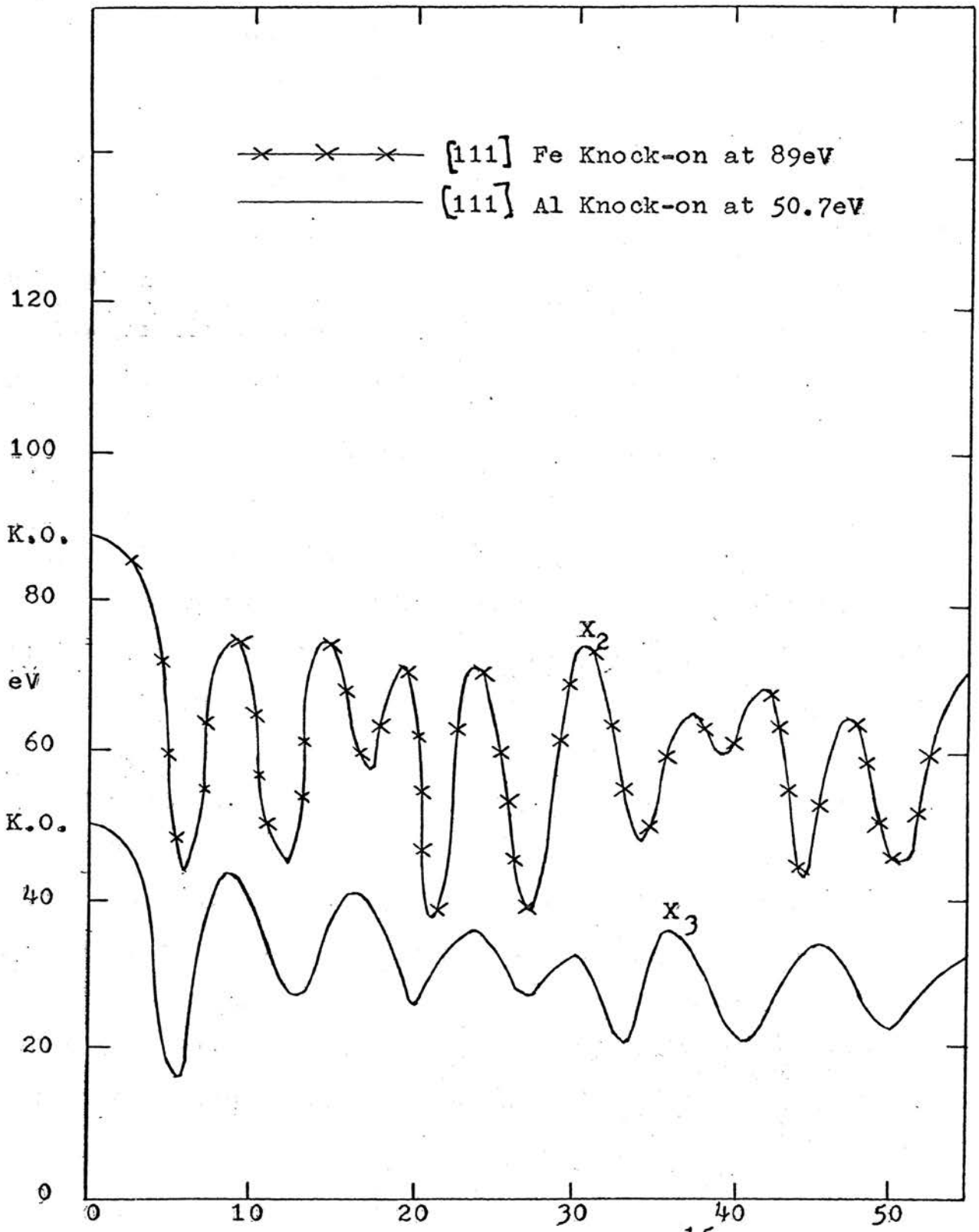

Attenuation of Kinetic Energy Pulse.
Figure 18

and about 6 eV was required in the 50 eV knock-on case.

For the purpose of illustration, the peak at X_2 (top of Figure 18) was assumed to be the first true maximum kinetic energy peak after the K.O. (knock-on) peak; then, by averaging over the 4 previous "apparent" maxima the kinetic energy lost per collision was found to be about .5 eV. When the same reasoning was applied to the bottom curve in Figure 18, at point X_3, the average kinetic energy lost per collision was found to be about 1.8 eV.

E. Focusing Collision in [111] Direction

Figure 19 shows the effect of an iron knock-on, A_4, (3,3,3) directed 1° above the [111] direction with a kinetic energy of 107 eV. Replacement collisions occurred at B_4 (4,4,4), C_4 (5,5,5), D_4 (6,6,6), E_4 (7,7,7), F_4 (8,8,8), and G_4 (9,9,9). Near the end of the collision chain (G_4, H_4 and I_4) the lattice structure in that area was expanded greatly with an interstitial formed in the neighborhood of G_4 and H_4. A vacancy was formed at A_4, while the neighboring lattice atoms (P_1 and P_2) relaxed slightly inward to help fill the void at A_4 created by the vacancy.

It is apparent from Figure 19 that a number of "focuson" mechanisms were evident in the [100] and [111] directions aiding the dissipation of energy from the collision chain.

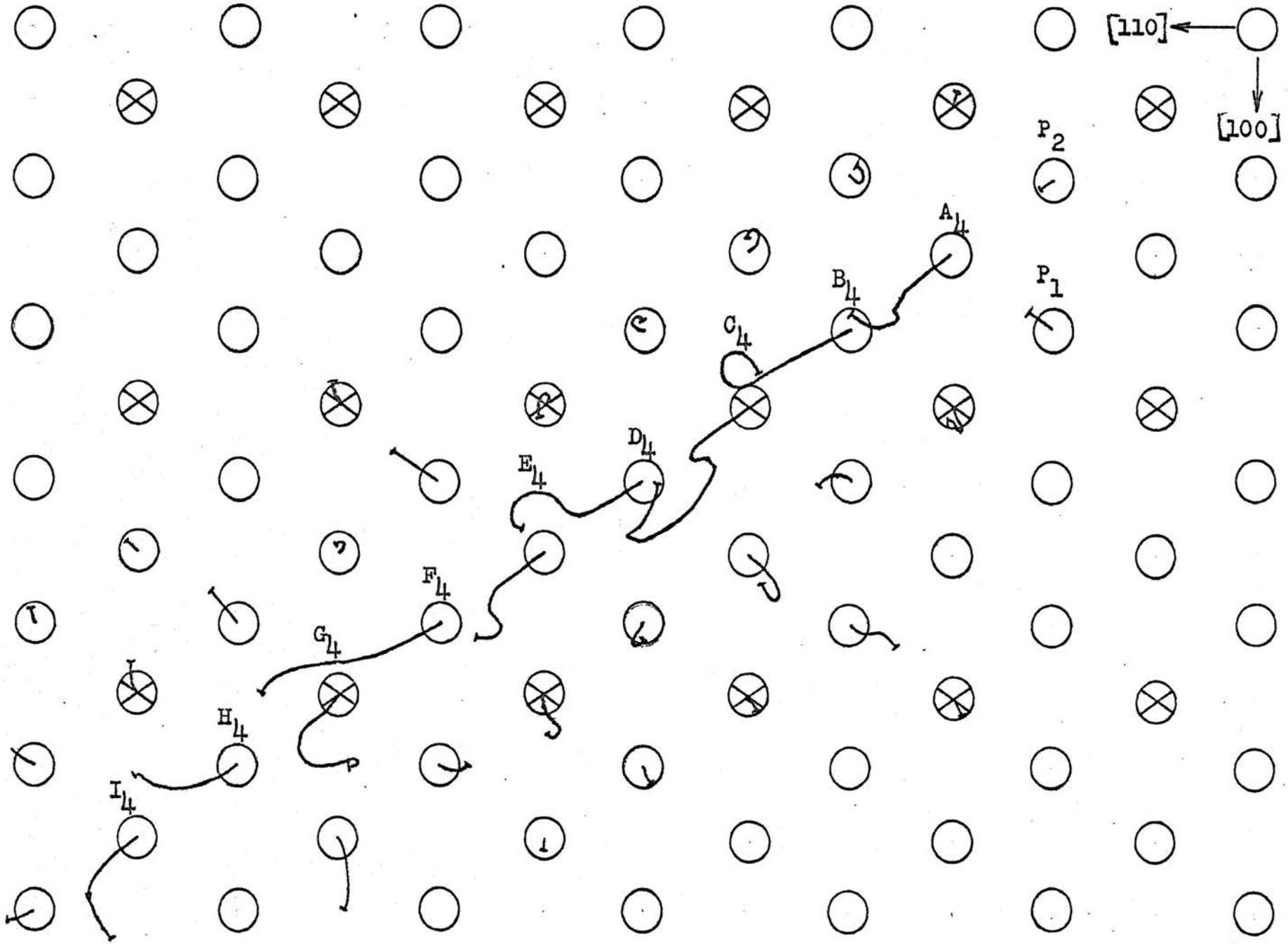

Figure 19 107 eV Fe Knock-on 1.0° from [111] Direction

Chapter V

DISCUSSION OF RESULTS

This was the first extensive computer study of Fe_3Al, or of any other ordered alloy, therefore the results of this study could not be compared directly to similar work. There were however a number of points in this investigation that could be compared with the work on pure copper by Gibson et al. (35) and especially pure alpha-iron by Erginsoy et al. (43).

It was evident from this investigation that the final damaged state, in all instances where the primary knock-on energy was above the threshold level, was composed primarily of Frenkel defects, vacancy-interstitial pairs. Also, the distance separating the vacancy and interstitial in a Frenkel pair was a sensitive function of the direction and energy of the primary knock-on. In only one case ([110]) Figure 10, was the primary knock-on ever found to go into an interstitial position rather, as in the cases of both pure copper and pure iron, the knock-on replaced another neighboring atom so that the interstitial originated down the collision chain.

In the [110] direction, Figure 10, the knock-on was

found to reside in a split interstitial configuration with a second atom as postulated by Erginsoy et al. for the alpha-iron. The center of gravity of the interstitial pair did not reside in the center of the potential well, as did Erginsoy's, but rather to the right of the point of intersection of the [111] axis and [110] collision chain as indicated by Erginsoy as the center of the split-interstitial that he proposed (see Figure 10). This configuration could not be considered as thoroughly stabilized, however, and a longer run may have shown the formation of a more site centered system.

The vacancy was also a normally stable configuration. The near neighbors relaxed inward to partially fill the void formed by the vacancy.

"Replacement chains" were very prevalent in the [100] and [110] directions and presented the primary method of matter transfer. An initial kinetic energy of about 11 eV (Figure 7) was lost furnishing the potential energy needed to initiate the replacement chain in the [100] direction (for a chain of all Fe atoms). Each of the [100] potential barriers formed by the 4 body-centered atoms surrounding the replacement chain absorbed about 5 eV compared with 5-6 eV obtained by Erginsoy et al. (43) for alpha-iron.

As in the case of iron and copper, the threshold energies needed to cause permanent atomic displacement in Fe_3Al were strongly dependent on the direction of knock-on. The

threshold energy for an iron atom in a [100] chain of all iron atoms was about 22 eV as compared to 17 eV for alpha-iron (from Erginsoy). For permanent displacement in the [110] direction, the atom had to pass through two barrier planes formed by the asymmetrical arrangement of atoms around the [110] axis; whereas, an atom displaced in the [100] direction needed to overcome only one barrier. The presence of two barriers caused the threshold energy to be substantially higher in the [110] direction than in the [100] direction; i.e., 44 eV as compared to 22 eV. In alpha-iron the [110] threshold was considerably lower - about 34 eV; however, in both the iron and Fe_3Al the threshold in the [110] direction was twice as high as that in the [100] direction, showing good agreement between the two systems.

In the [100] direction most of the kinetic energy pulse remained in the collision chain with very little being lost to the atoms surrounding the chain (about 5 eV per potential barrier). In the [110] direction, however, much of the energy was "drained" from the replacement chain by a series of "focusons" in the [110] (Figure 10) and [111] (Figure 19) directions. The focusons transferred energy but no matter away from the chain. This energy dissipation in a rather small volume, without matter transport, might be likened to the "thermal spike" concept proposed by Seitz (15). The same form of energy drain occurred in both chains of all

iron (Figure 10) and all aluminum atoms in the [110] direction.

The results discussed above agree, in general, with the results of studies on copper, and iron, even though this study employed a model of an alloy Fe_3Al. This similarity arose from the fact that the collision chains studied in the [100] and [110] directions contained either all iron or all aluminum atoms with no mixing of the two species. The discussion below will show the poor agreement between this study and previous studies when the primary dynamic event involves both iron and aluminum atoms.

All [111] (Figures 12, 13, 14, 15) chains contained aluminum atoms separated by three iron atoms. This mixed structure greatly increased the complexity of the dynamic events.

It was expected that the close-packed nature of the [111] direction would necessitate a higher threshold energy for permanent displacement. Erginsoy et al. found that in alpha-iron this threshold was about 38 eV, or a little higher than that for the [110] direction.

No definite threshold could be determined for the [111] direction in Fe_3Al, since the character of the dynamic processes was strongly dependent on the relative location of the aluminum atoms with respect to the knock-on atom. It was found that, irrespective of the starting atom, the knock-on was never permanently displaced (even at energies of 89 eV).

The series of collision chains initiated at an energy of about 50 eV at various locations along the [111] axis indicated the most extensive motion along the collision chain occurred when the primary knock-on, or the first atom in the chain, was an iron atom followed by an aluminum as the second atom in the chain (Figure 15).

Replacement collisions occurred only at higher energies (about 89 eV) and the vacancy was not formed at the original site of the knock-on, but rather several lattice distances further along the chain.

The above results indicated that the presence of both iron and aluminum atoms in the same chain was responsible for the lack of agreement between this and previous investigations on pure iron. The aluminum atom has about half the mass of the iron atom and, thus, for the same kinetic energy the aluminum atom had a higher velocity.

At relatively low kinetic energies the iron atoms forming the lattice had a chance to relax and begin their forward motion, thus, lowering the kinetic energy needed to cause permanent displacement of the aluminum knock-on. Theoretically, the aluminum atom could impart a maximum of about 88% of its kinetic energy to the iron atom occupying the lattice site immediately following the aluminum knock-on in the chain. It was concluded from the results of this investigation that at energies sufficiently low to allow the iron lattice to relax the aluminum atom could not transfer sufficient energy

to the iron "second" atom to propagate a replacement chain.

At higher energies the iron lattice did not have sufficient time to relax before the aluminum atom had reached the point of closest approach between the iron and aluminum atom; and, thus, the threshold energy needed by the aluminum atom was higher than normal. It was apparent from these results that the degree of relaxation of the lattice ahead of a displaced atom had a strong effect on the energy needed to propagate a replacement chain.

A chain of billiard balls might represent a helpful analogy. It is apparent that striking the first billiard ball along the axis of the chain would correspond to a primary knock-on, and the subsequent motion of the chain of billiard balls would closely resemble a replacement chain.

It is also apparent, from classical physics, that the presence of a golf ball in the chain would impede the transfer of kinetic energy and, thus, the progress of the replacement process. If the knock-on in this analogy were the golf ball and not the billiard ball, and if this were the only golf ball present in the chain, it would be anticipated that the replacement chain would propagate normally, as though the knock-on were indeed a billiard ball, if and only if the kinetic energy of the golf ball were sufficiently great.

In the light of the above analogy, the presence of aluminum atoms along the [111] chain in every fourth lattice site would greatly impede the formation of an extensive

replacement chain. It might thus be assumed that a larger initial kinetic energy would be needed to initiate a replacement chain in Fe_3Al than was observed in pure iron. From the results of this investigation, it was apparent that this was indeed the case.

Several attempts were made to investigate the effects of directing knock-ons at small angles (about 1.0 to 1.5°) to the major axis. In all cased the knock-on energy was in the range of 110 eV and "defocusing" was observed to occur as the replacement chain progressed (Figures 8, 9, 19). From the earlier results of Erginsoy et al. (43) on alpha-iron, it was assumed that the defocusing was partially produced by the rather high energy of the primary knock-on. Erginsoy et al. found that for angles of less than 10° focusing occurred in the [111] direction, for energies less than 28 eV and in the [100] direction for energies less than 18 eV.

In the Fe_3Al alloy additional defocusing was always caused by the presence of aluminum atoms in the replacement chain, in the [111] case (Figure 19) or as near neighbors to the chain in the [100] case (Figure 8). The [111] replacement chains showed the largest degree of defocusing when aluminum atoms were involved. This, again, was the result of the small mass of the aluminum atom relative to that of the iron. The lighter aluminum atom tended to be displaced from its normal lattice site more easily and to a

larger extent than the iron atoms.

When the collision chain was surrounded by alternate iron and aluminum atoms, such as in the [100] direction, the defocusing, that was initiated originally in the [100] (Figure 8) plane tended to rotate into the [110] plane where the aluminum atoms reside because of their ease of motion.

An interesting phenomenon associated with defocusing was a lattice expansion about the axis of the replacement chain. The loss of energy through this small expansion was, again, assumed to be related to a type of "thermal spike" phenomenon. This mechanism was apparent through the [100] defocused replacement chain and the early stages of the [111] defocused replacement chain. At the end of the [111] (Figure 19) collision chain, there was a sudden gross expansion of the lattice as the remainder of the kinetic pulse was dissipated in all directions in the lattice. This expansion was comparable to the "plastic spike" postulated by Seitz to be associated with a thermal spike.

The majority of the collision chains in the [100] and [110] direction contained chains of either all aluminum or all iron atoms and thus very little disordering was observed. It was postulated that the largest amount of disordering would occur in the [111] direction with both iron and aluminum atoms present. The replacement chain was very difficult to initiate and to propagate, so that the amount

of disordering was very small, at least to energies of about 89 eV.

The largest amount of disordering occurred in the defocused chains; especially, in the [111] direction (Figure 19). This disordering was attributed to the random mixing of the lattice near the end of the collision chain.

Chapter VI

CONCLUSIONS

From the results of this investigation on the ordered alloy Fe_3Al, the following conclusions were arrived at:

1. The final damaged state after irradiation at or near threshold levels is composed primarily of Frenkel defects; vacancy-interstitial pairs.

2. The primary mechanism for the formation of Frenkel defects and for separating the vacancy and interstitial is the "replacement chain." By this mechanism a large number of replacements may be produced per single displacement especially in the [100] direction. An initial energy loss of about 10-15 eV is needed to initiate the replacement chain, but after initiated, the chain progresses with much less energy loss.

3. The vacancy is a normal stable defect; and the interstitial resides in the [110] direction in a split-interstitial configuration. Unlike the split-interstitial in alpha-iron, proposed by Erginsoy et al. (43), the center of gravity of the pair does not lie at the center of symmetry formed by the [111] axis but rather displaced slightly to the right. This may not be the final stable

state, since time was not available to allow the system to become perfectly stable.

4. The threshold energy for permanent atomic displacement is strongly directionally dependent. The threshold in the [100] direction (all Fe atoms) is 22 eV and that in the [110] direction (either all Fe or all Al) is 44 eV. The presence of both iron and aluminum atoms along the [111] axis precluded the determination of a single exact threshold energy. The form that the collisions chain takes in the [111] direction is strongly dependent on the location of the aluminum atom relative to the primary knock-on.

The results of the runs in the [111] direction may be partly explained using a billiard ball and golf ball analogy. Although no single threshold was determined for the [111] direction, it is concluded that it must be substantially higher than that for either the [100] or [110] directions.

5. Defocusing is found to occur for knock-ons directed from 1.0° to 1.5° away from the major axis at an energy of about 110 eV. The loss of energy in the early stages of the defocused replacement chain is related to the "thermal spike" concept of Seitz (15). Also the relatively large expansion of the lattice at the end of the [111] defocused replacement chain is similar to the "plasticity spike" also proposed by Seitz.

The aluminum atoms play a prominent role in increasing

the degree of focusing in the [100] and [111] directions.

6. Unlike the reports of Vineyard (44) (of large amounts of disordering in Cu_3Au) the amount of disordering seen in Fe_3Al in this study is very small. Disordering is only prevalent in the [100] and [111] defocusing runs where a large amount of atomic mixing occurs near the end of the replacement chains.

Since the [100] and [110] replacement chains (without defocusing) were composed of only one atomic species, the replacement mechanism does not lead to disordering.

7. The "focuson" is a very important mechanism for dissipating energy from both replacement chains and defocused replacement chains. This is especially true in the [110] replacement chains where focusons in the [100] and [111] directions help dissipate energy.

Chapter VII

RECOMMENDATIONS

The following set of studies should be made:

1. A complete series of runs in directions off the major diagonals at a variety of energies to determine focusing-defocusing properties of the Fe_3Al lattice;

2. Higher energy runs in the [111] direction starting at various knock-on locations to determine a complete picture of the effect of aluminum atoms on the [111] collision events; and

3. Single crystal experiments on Fe_3Al to check on threshold energies and other results of this study.

4. Investigation of the stability of various point defects; such as the vacancy, interstitial, split-interstitial, crowdion, etc.

APPENDIX

APPENDIX A

Computer Program and Input Data

A. Computer Program

```
C       REVISION OF GRAPE 1 PROGRAM
C       PROGRAM FOR FE 3 AL LATTICE
C       PROGRAM SETS UP B.C.C. CRYSTAL
C
C
     1 FORMAT(I15)
     4 FORMAT(4E15.4)
     5 FORMAT(E15.4)
     6 FORMAT(3E15.4)
     7 FORMAT(I15,3E15.4)
     9 FORMAT(I5,I2,I2,I4,5I2)
    17 FORMAT (F15.8)
    18 FORMAT (I15)
    19 FORMAT (3I15)
    50 FORMAT(8H1GRAPE  ,I7,20X,I2,1H/,I2,1H/,I4,21X,4HPAGE,I3)
    52 FORMAT (I6,3F15.4,2I10)
    53 FORMAT(//4X,3HBND,10X,1HA,15X,1HB,15X,1HC)
    54 FORMAT(I6,3E15.4)
   800 FORMAT(24I3)
   904 FORMAT(3F15.4,I15)
       COMMON BOX(4096),AC(3),IBND(1000),E(1001),X(1000,3),
      1F3(1001),IAUX(27),IDUX(27),J,L,I,L2,IGAM,BBOX,XX,YY,
      2E2,H,F,ENGPO,ZZ1(1000),ZZ2(1000),ZZ3(1000),A1(3)
      3,F1(1001),EE2(1001),F2(1001),EE3(1001),IMNT,IK(2735),
      4ZZ,RR,E1,B1(3),EE1(1001)
       DIMENSION A(50,3),B(50,3),C(50,3),V(1000,3),TB(1000,3),
      1DTN(6),KAC(1000),IIB(27),INV(99,3),IV(99),D(3),XM(3)
      2,A2(50,3),B2(50,3),C2(50,3),TT(6)
       T=0.0
       ENGKE=0.0
C      THERE ARE 27 BOUNDARY CONDITIONS, 26 FOR ATOMS
C      LOCATED AT DIFFERENT PLACES ON THE SURFACE AND ONE
C      FOR AN ATOM IN THE INTERIOR
C      BOUNDARY CONSTANTS
       DATA IIB(1),IIB(2),IIB(3),IIB(4),IIB(5),IIB(6),IIB(7),
      1IIB(8),IIB(9),IIB(10),IIB(11),IIB(12),IIB(13),IIB(14),
      IIIB(15),IIB(16),IIB(17),IIB(18),IIB(19),IIB(20),IIB(21),
      3IIB(22),IIB(23),IIB(24),IIB(25),IIB(26)/1,4,2,15,17,5,16,
      418,3,11,13,7,19,20,9,21,25,6,12,14,8,22,24,10,23,26/
       DO 8 I=1,1000
       DO 8 J=1,3
     8 V(I,J)=0.0
C      INITIAL PARTICLE VELOCITIES INTRODUCED
       NTIN=1
       NTPR=3
       NTPU=2
       NTTEMP=18
       READ (1,9)IPROB,MONTH,KAY,IEAR,IA,IB,IC,NV,NR
       WRITE (3,9) IPROB,MONTH,KAY,IEAR,IA,IB,IC,NV,NR
       IALP=IA+2
       IBET=(IA+2)*(IB+2)
       IGAM=(IBET)*(IC+2)
C      ARE THERE ANY VACANCIES
       IF(NV)801,802,801
```

```
C       COMBINE 3-COORDINATES INTO 1-COORDINATE
  801   READ (NTIN,800) ((INV(K,J),J=1,3),K=1,NV)
        DO 803 J=1,NV
  803   IV(J)=900*INV(J,1)+30*INV(J,2)+INV(J,3)
  802   CONTINUE
C       DETERMINE POSSIBLE NUMBER OF ATOMS
        IE1=IA/2+1
        IO1=(IA+1)/2
        IE2=IB/2+1
        IO2=(IB+1)/2
        IE3=IC/2+1
        IO3=(IC+1)/2
C       N IS THE TOTAL NUMBER OF ATOMS IN THE CRYSTAL
        N=(IE1*IE2*IE3)+(IO1*IO2*IO3)-NV+NR
        K1=IA+1
        K2=IB+1
        K3=IC+1
        WRITE (3,19) K1,K2,K3
        K12=K1-2
        K22=K2-2
        K32=K3-2
        L=1
C       GENERATING CRYSTAL
        DO 3 I1=1,K1
C       IS THIS AN ODD OR AN EVEN PLANE
        IF (I1/2*2-I1) 102,161,102
C       SET UP FOR I1 ODD
  102   KK1=1
        GO TO 103
C       SET UP FOR I1 EVEN
  161   KK1=2
  103   DO 3 I2=KK1,K2,2
        DO 3 I3=KK1,K3,2
    2   IF (NV) 804,805,804
  804   DO 806 J=1,NV
C       IN ORDER TO USE ONE NUMBER TO DESCRIBE THE LOCATION
C       OF AN ATOM, THE COORDINATES ARE COMBINED INTO ONE NO.
C       COMBINE 3-COORDINATES INTO ONE COORDINATE
        KV=900*(I1-1)+30*(I2-1)+I3-1
C       SEARCH VACANCY 1-COORDINATE TABLE
        IF (KV-IV(J)) 806,807,806
  807   GO TO 3
  806   CONTINUE
  805   CONTINUE
C       DETERMINE BOUNDARY TYPE
        M=2*((I3+K3)/(2*K3))+(K3-I3+1)/K3+(2*((I2+K2)/(2*K2))+
       1(K2-I2+1)/K2)*3+(2*((I1+K1)/(2*K1))+(K1-I1+1)/K1)*9
C       STORE COORDINATE IN X-TABLE
        IF(M) 500,600,500
  600   I12=I1-1
        I22=I2-1
        I32=I3-1
        M=2*((I32+K32)/(2*K32))+(K32-I32+1)/K32
       1+(2*((I22+K22)/(2*K22))+(K22-I22+1)/K22)*3
```

```
     2+(2*((I12+K12)/(2*K12))+(K12-I12+1)/K12)*9
      IF (M) 501,502,501
  501 M=-IIB(M)
      GO TO 502
  500 M=IIB(M)
  502 X(L,1)=I1-1
      X(L,2)=I2-1
      X(L,3)=I3-1
C     THE TABLE IBND GIVES THE BOUNDARY CONDITION FOR EACH ATOM
      IBND(L)=M
      L=L+1
    3 CONTINUE
C     READ IN REPLACEMENTS AND STORE AT END OF X-TABLE
      M1=N-NR+1
      M=N+1
      IF (M1.EQ.M) GO TO 905
      DO 808 I=M1,N
  808 READ (NTIN,904) (X(I,J),J=1,3),IBND(I)
      WRITE (3,904) (X(I,J),J=1,3),IBND(I)
C     TEST FOR BOUNDARY ATOMS
C     IF BOUNDARY STORE COORDINATE IN TB TABLE
  905 DO 10 I=1,N
      IF(IBND(I)) 20,10,20
   20 MM=I
      DO 21 J=1,3
   21 TB(I,J)=X(I,J)
   10 CONTINUE
C     IN THE SRHBX TECHNIQUE AN ARRAY IAUX IS SET UP TO
C     DETERMINE THE COORDINATES OF THE FIRST NEIGHBOR BOX TO BE
C     SEARCHED. THE LENGTH OF THE TABLE IS IDUX
C     SET UP NEIGHBOR SEARCH TABLES
      I=1
      DO 1192 I1=1,3
      DO 1192 I2=1,3
      DO 1192 I3=1,3
C     SET UP MINIMUM VALUES
      L1=1-(3*(I1-1)*(I1-3))
      L2=1-(3*(I2-1)*(I2-3))
      L3=1-(3*(I3-1)*(I3-3))
C     DETERMINE MAXIMUM VALUES
      M1=(14-3*(I1-1)*(I1-2))/2
      M2=(14-3*(I2-1)*(I2-2))/2
      M3=(14-3*(I3-1)*(I3-2))/2
      J1=I
C     DETERMINE BOUNDARY TYPE
      J=I3-1+3*(I2-1)+9*(I1-1)
      IF (J) 1193,1194,1193
 1194 M=1
      GO TO 1195
 1193 M=IIB(J)+1
C     ENTRY TO TABLE
 1195 IAUX(M)=I
C     SET UP SEARCH TABLE FOR THIS BOUNDARY TYPE
      DO 1191 K1=L1,M1
```

```
      DO 1191 K2=L2,M2
      DO 1191 K3=L3,M3
C     CRITERION_ COORDINATE SUM LESS OR EQUAL TO 6
      IF (IABS(K1-4)+IABS(K2-4)+IABS(K3-4)-6) 1190,1190,1191
 1190 IK(I)=K1+IALP*K2+IBET*K3-4*(1+IALP+IBET)
      I=I+1
 1191 CONTINUE
C     LENGTH OF TABLE
 1192 IDUX(M)=I-J1
C     COMPUTE FORCE AND POTENTIAL TABLE
      READ (NTIN,4) AA,BB,RMIN,RMAX
      WRITE (3,4) AA,BB,RMIN,RMAX
      READ (1,33) ((A1(I),B1(I)),I=1,3)
   33 FORMAT (2F10.6)
      DO 1113 I=1,1001
      EE1(I)=0.0
      F1(I)=0.0
      EE2(I)=0.00
      F2(I)=0.0
      EE3(I)=0.0
 1113 F3(I)=0.0
C     POTENTIAL FUNCTIONS BEING GENERATED AND STORED
      RO=2.0000
      DO 11 J=1,3
      XX=RMIN**2
      H=(RMAX**2-XX)/999.0
      IF(J-3) 1201,1205,1205
 1201 IF (J-2) 1203,1204,1203
 1203 IF (J-1) 1202,1202,1202
C      THIS IS A MORSE TYPE POTENTIAL
 1202 XX=RMIN**2
      DO 313 I=1,1000
      EEE=(A1(J)*((EXP(-2.0*B1(J)*(SQRT(XX)-RO)))-2.0*EXP(-B1(J)
     1*(SQRT(XX)-RO))))
      EE3(I)=EE3(I)+EEE
      F3(I)=(A1(J)*(-2.0*B1(J)*(EXP(-2.0*B1(J)*(SQRT(XX)-RO)))
     1+2.0*B1(J)*EXP(-B1(J)*(SQRT(XX)-RO))))/(SQRT(XX))
      F3(I)=-F3(I)
  313 XX=XX+H
      GO TO 11
C     THIS IS A BORN MAYER POTENTIAL
 1204 XX=RMIN**2
      DO 312 I=1,1000
      EEE=(A1(J)*(EXP(-B1(J)*SQRT(XX))))/B1(J)
      EE2(I)=EE2(I)+EEE
      F2(I)=F2(I)+(EEE*B1(J))/SQRT(XX)
  312 XX=XX+H
      GO TO 11
C     THIS IS A SCREENED POTENTIAL
 1205 XX=RMIN**2
      DO 311 I=1,1000
      EE1(I)=EE2(I)*(0.7)/SQRT(XX)
      F1(I)=F2(I)*(0.7)/SQRT(XX)
  311 XX=XX+H
```

```
   11 CONTINUE
 1116 E2=((-RMIN**2)/H)+1.
      E1=1./H
      READ (NTIN,5) DT
      WRITE (3,5) DT
      READ (NTIN,1) M
      WRITE (3,1) M
      RVT=0.46325
      DO 12 J=1,3
      DO 12 I=1,M
      READ (NTIN,6) A(I,J),B(I,J),C(I,J)
   12 A(I,J)=+A(I,J)/RVT
C     TEST TO SEE IF PARTICLE IS ALUMINUM OR IRON
      READ (NTIN,1) MOV
      DO 118 I=1,N
      MMM=X(I,1)+X(I,2)+X(I,3)
      MTD=MOD(MMM,4)
C     IF MTD IS THREE THEN THE ATOM IS AN ALUMINUM
      IF (MTD-3) 15,16,15
C     SET UP TABLE DENOTING TYPE OG PARTICLE
   15 KAC(I)=-1
      GO TO 118
   16 KAC(I)=0
  118 CONTINUE
      READ (1,1120) (XM(J),J=1,3)
 1120 FORMAT (3F15.4)
      READ (NTIN,7) L,D(1),D(2),D(3)
      WRITE (3,7) L,D(1),D(2),D(3)
      DO 1121 I=1,MOV
      IF (KAC(L)) 4000,4001,117
  117 WRITE (3,171)
  171 FORMAT (19H1ERROR IN KAC TABLE)
      CALL EXIT
 4000 ENGKE=ENGKE+1.04*(D(1)**2+D(2)**2+D(3)**2)
      GO TO 4002
 4001 ENGKE=ENGKE+.5*(D(1)**2+D(2)**2+D(3)**2)
 4002 N1=N+1
      DO 1121 J=1,N1
      IF (XM(1)-X(J,1)) 1123,1122,1123
 1122 IF (XM(2)-X(J,2)) 1123,1124,1123
 1124 IF (XM(3)-X(J,3)) 1123,1125,1123
 1125 DO 1126 K=1,3
 1126 V(J,K)=D(K)
      GO TO 1121
 1123 CONTINUE
 1121 CONTINUE
C     CHOOSE CENTER OF CRYSTAL AS ABOUT 4,4,4
C     DETERMINATION OF DISTANCE SEPARATING ANY GIVEN ATOMS
C     SHOULD APPEAR HERE
 1901 FORMAT (3X,4HDIF=,2X,F10.4,2X,4HKAC=,2X,I5,2X,I5)
      DO 14 I=1,N
      DO 14 J=1,3
   14 V(I,J)=(V(I,J)*DT)+X(I,J)
      IP=1
```

```
      WRITE (3,90) T,IPROB,MONTH,KAY,IEAR,N,M,DT,E1,E2,MM,IP
      INSEN=0
      DO 35 I=1,27
   35 WRITE (3,96) I,IAUX(I),IDUX(I)
      WRITE (3,98) IALP,IBET,IGAM,ENGKE
   60 IP=1
   68 CO=50.0
      DO 63 I=1,N
      IF (50.-CO) 61,61,62
   61 WRITE (3,50) IPROB,MONTH,KAY,IEAR,IP
      IP=IP+1
      WRITE (3,51)
      CO=0.0
   62 WRITE (3,52) I,X(I,1),X(I,2),X(I,3),IBND(I),KAC(I)
      CO=CO+1.0
   63 CONTINUE
      DO 64 J=1,3
      WRITE (3,50) IPROB,MONTH,KAY,IEAR,IP
      IP=IP+1
      WRITE (3,53)
      DO 64 I=1,M
   64 WRITE (3,7) I,A(I,J),B(I,J),C(I,J)
   90 FORMAT (E15.4,I5,I2,I2,I4,2I5,3E15.4,2I4)
   91 FORMAT (//,3HX= ,E15.8,2X,3HY= ,E15.8,2X,I5,I5)
   92 FORMAT (//,4HTB= ,//,E15.8,2X,I5,2X,I5)
   94 FORMAT (//,2HN=,2X,I5,3X,5HIBND=,2X,I5)
   95 FORMAT (//,2HE=,2X,E15.8,2X,3HEE=,2X,E15.8)
   96 FORMAT (//,I5,2X,5HIAUX=,I5,2X,5HIDUX=,I5)
   97 FORMAT (//,3HIK=,2X,10I5)
   98 FORMAT (//,5HIALP=,I5,2X,5HIBET=,I5,2X,5HIGAM=,I5,2X,
     16HENGKE=,E15.4)
C      GRAPE CODE CGRZIOB PART 2
C      GRAPE PART 2 REVISED FOR FINAL TIME FOR B.C.C. OF
C      TWO MASSES
 3051 FORMAT (1H ,7F15.6)
 3050 FORMAT (6(F7.2,F5.2))
 4052 FORMAT (23H1BEGIN PROCESSING GRAPE,1X,I4,5X,I2,1H/,
     1I2,1H/,I4)
 4050 FORMAT (21HNORMAL END OF PROGRAM)
 4051 FORMAT(' PROGRAM BEING TERMINATED DUE TO TOO LARGE',
     1' A DISCREPANCY AT T=',F9.3)
 4053 FORMAT (22H PROGRAM RAN THRU T = ,F9.3,
     131H AND DT IS NOW BEING CHANGED TO,F7.3)
C      READ INPUT TAPE
      READ(1,3050) (TT(I),DTN(I),I=1,6)
      DO 333 I=1,6
  333 WRITE (3,3333) TT(I),DTN(I)
 3333 FORMAT (2X,2F7.2)
      NT=1
C      INITIALIZE TIME STEP COUNT
      INO1=1
C      SET TOLERANCE
      TOL=20.0
      E(1001)=0.
```

```
C       READ INITIAL 5 RECORDS
        WRITE (3,4052) IPROB,MONTH,KAY,IEAR
        ENGKE=2000.*ENGKE
        ENGLO=0.
        K=1
        INSEN=1
C       WE ARE ASSUMING SECOND LAYER FORCES SMALL
        DO 9900 I=1,M
        DO 9900 J=1,3
        A2(I,J)=+0.000
        B2(I,J)=B(I,J)/200.0
 9900   C2(I,J)=0.000
  903   DDT=DT*DT
        DO 1004 I=1,M
        DO 1004 J=1,3
        C2(I,J)=C2(I,J)/DT
 1004   C(I,J)=C(I,J)/DT
 9991   FORMAT (2X,2HC=,2X,E15.4)
C       TIME STEP INITIALIZATION
  101   DO 115 I=1,4096
  115   BOX(I)=0.
        ENGL=0.
        ENGKG=0.
        ENGPO=0.
        ENGSP=0.
C       SETUP TABLE BOX(J), J DETERMINED BY COORDINATE
C       BOX CONTAINS PARTICLE NUMBER
C       THIS PLACES EACH OF THE PARTICLES IN A BOX
C       THAT THE CRYSTAL HAS BEEN DIVIDED INTO
        DO 111 I=1,N
        LX=X(I,1)+1.5
        LY=X(I,2)+1.5
        LZ=X(I,3)+1.5
        J=LX+IALP*LY+IBET*LZ-IALP-IBET
        L=I
        CALL SETBX
  111   CONTINUE
C       INITIALIZE PARTIAL ACCELERATION SUMS
        DO 211 I=1,1000
        ZZ1(I)=0.0
        ZZ2(I)=0.0
  211   ZZ3(I)=0.0
        DO 431 I=1,N
        L=I
        I=L
C       CALCULATE NEIGHBOR CONTRIBUTION TO ACCELERATION
C       AND POTENTIAL ENERGY OF PAIR FORCES
        CALL SRHBX
C       IF PARTICLE IS ON BOUNDARY CALCULATE
C       BOUNDARY INFLUENCE
C       RATIO OF ATOMIC MASSES = RAT
        RAT=2.07
   37   IF (IBND(I)) 40,420,401
   40   L=-IBND(I)
```

```
      ENGL=ENGL-((V(I,1)-X(I,1))**2)*C2(L,1)-((V(I,2)-X(I,2))**2)
     1*C2(L,2)-((V(I,3)-X(I,3))**2)*C2(L,3)
  444 FORMAT (2X,5HENGL=,2X,E15.4)
      DX=X(I,1)-TB(I,1)
      DY=X(I,2)-TB(I,2)
      DZ=X(I,3)-TB(I,3)
      ENGSP=ENGSP-A2(L,1)*DX-A2(L,2)*DY-A2(L,3)*DZ-.5*
     1(B2(L,1)*(DX**2)+B2(L,2)*(DY**2)+B2(L,3)*(DZ**2))
  555 FORMAT (2X,6HENGSP=,2X,E15.4)
  678 FORMAT (2X,3E18.4,I10)
      AC(1)=AC(1)+A2(L,1)+DX*B2(L,1)+(V(I,1)-X(I,1))*C2(L,1)
      AC(2)=AC(2)+A2(L,2)+DY*B2(L,2)+(V(I,2)-X(I,2))*C2(L,2)
      AC(3)=AC(3)+A2(L,3)+DZ*B2(L,3)+(V(I,3)-X(I,3))*C2(L,3)
C     IS THIS PARTICLE IRON OR ALUMINUM
  420 IF (KAC(I)) 430,43,43
  430 V(I,1)=(2.0/RAT)*(AC(1)*DDT)+2.0*V(I,1)-X(I,1)
      V(I,2)=(2.0/RAT)*(AC(2)*DDT)+2.0*V(I,2)-X(I,2)
      V(I,3)=(2.0/RAT)*(AC(3)*DDT)+2.0*V(I,3)-X(I,3)
      GO TO 431
   43 V(I,1)=(AC(1)*DDT+V(I,1))+(AC(1)*DDT+V(I,1))-X(I,1)
      V(I,2)=(AC(2)*DDT+V(I,2))+(AC(2)*DDT+V(I,2))-X(I,2)
      V(I,3)=(AC(3)*DDT+V(I,3))+(AC(3)*DDT+V(I,3))-X(I,3)
      GO TO 431
  401 L=IBND(I)
C     CALCULATE VARIOUS ENERGIES AND CHECK DISCREPANCY
      ENGL=ENGL-((V(I,1)-X(I,1))**2)*C(L,1)-((V(I,2)-X(I,2))**2)
     1*C(L,2)-((V(I,3)-X(I,3))**2)*C(L,3)
      DX=X(I,1)-TB(I,1)
      DY=X(I,2)-TB(I,2)
      DZ=X(I,3)-TB(I,3)
      ENGSP=ENGSP-A(L,1)*DX-A(L,2)*DY-A(L,3)*DZ-.5*(B(L,1)
     1*(DX**2)+B(L,2)*(DY**2)+B(L,3)*(DZ**2))
  676 FORMAT(4E18.4)
  677 FORMAT(3E18.4)
      AC(1)=AC(1)+A(L,1)+DX*B(L,1)+((V(I,1)-X(I,1)))*C(L,1)
      AC(2)=AC(2)+A(L,2)+DY*B(L,2)+((V(I,2)-X(I,2)))*C(L,2)
      AC(3)=AC(3)+A(L,3)+DZ*B(L,3)+((V(I,3)-X(I,3)))*C(L,3)
      IF(KAC(I)) 422,42,42
  422 V(I,1)=(2.0/RAT)*(AC(1)*DDT)+2.0*V(I,1)-X(I,1)
      V(I,2)=(2.0/RAT)*(AC(2)*DDT)+2.0*V(I,2)-X(I,2)
      V(I,3)=(2.0/RAT)*(AC(3)*DDT)+2.0*V(I,3)-X(I,3)
      GO TO 431
   42 V(I,1)=(AC(1)*DDT+V(I,1))+(AC(1)*DDT+V(I,1))-X(I,1)
      V(I,2)=(AC(2)*DDT+V(I,2))+(AC(2)*DDT+V(I,2))-X(I,2)
      V(I,3)=(AC(3)*DDT+V(I,3))+(AC(3)*DDT+V(I,3))-X(I,3)
  431 CONTINUE
      DO 45 I=1,N
      X(I,1)=(V(I,1)+X(I,1))*.5
      X(I,2)=(V(I,2)+X(I,2))*.5
      X(I,3)=(V(I,3)+X(I,3))*.5
      EK1=V(I,1)-X(I,1)
      EK2=V(I,2)-X(I,2)
      EK3=V(I,3)-X(I,3)
C     IS THIS PARTICLE OF DIFFERENT MASS
```

```
      IF(KAC(I))4009,4008,4008
 4008 ENGKG=ENGKG+(EK1**2+EK2**2+EK3**2)
      GO TO 45
 4009 ENGKG=ENGKG+RAT*(EK1**2)+RAT*(EK2**2)+RAT*(EK3**2)
   45 CONTINUE
      NN=144
      ENKE1=(V(NN,1)-X(NN,1))**2+(V(NN,2)-X(NN,2))**2+
     1(V(NN,3)-X(NN,3))**2
      ENKE1=RAT*ENKE1
      ENKE1=1000.0*ENKE1/DDT
      WRITE (3,590) ENKE1
  590 FORMAT (2X,24HKENETIC ENERGY KNOCK ON=,E15.4)
      WRITE (3,666) ENGKG
  666 FORMAT (2X,6HENGKG=,2X,E15.4)
      ENGPO=ENGPO*2000.
      ENGSP=ENGSP*2000.
      ENGKG=(1000.*ENGKG)/DDT
      ENGKA=.5*(ENGKG+ENGKE)
      ENGKE=ENGKG
      ENGLO=ENGL*2000.+ENGLO
      LL=MOD(K,2)
      IF (LL) 3000,3000,2000
 2000 ENGTO=ENGKA+ENGPO+ENGSP
 3000 DESCR=ENGTO-ENGKA-ENGSP-ENGPO-ENGLO
      WRITE (3,777) DESCR
  777 FORMAT (2X,6HDESCR=,2X,E15.4)
      ENGTO=ENGTO-DESCR
      T=T+DT
      WRITE (3,3051) T,ENGKA,ENGPO,ENGSP,ENGLO,ENGTO,DESCR
      K=K+1
C     TEST DISCREPANCY
      TOL1=ABS(DESCR)
      IF (TOL1-TOL) 3007,3007,3002
 3007 LL=MOD(K,4)
      IF (LL) 3012,3012,3011
 3011 CONTINUE
      INO1=INO1+1
C     TEST FOR EVEN OR ODD TIME STEP
C     EVEN TIME STEP
C     IS RUN TO BE ENDED OR DT CHANGED
      IF (TT(NT)-T) 4100,4100,2010
 4100 IF (DTN(NT)) 2010,2011,2010
C     END RUN
 2011 INSEN=0
 2010 CONTINUE
      DO 299 I=1,N
  299 WRITE (3,566) I,V(I,1),V(I,2),V(I,3),IBND(I),X(I,1),
     1X(I,2),X(I,3),I
  566 FORMAT (I6,2X,3HVX=,E12.4,2X,3HVY=,E12.4,2X,3HVZ=,
     1E12.4,2X,I4,2X,3F12.4,2X,I6)
      WRITE(3,76) IPROB,MONTH,KAY,IEAR,T,N
      WRITE (3,3051)DT,ENGKA,ENGPO,ENGSP,ENGLO,ENGTO,DESCR
      WRITE (3,3051) ENGKE,EGKA1,EGPO1,EGSP1,EGLO1,EGTO1,DSCR1
      WRITE (3,1111) INSEN
```

```
      IF (TT(NT)-T) 4101,4101,101
 4102 WRITE (3,4050)
 3005 CALL EXIT
C     TEST FOR DT CHANGE OR END OF RUN
 4101 IF (DTN(NT)) 1000,4102,1000
 1000 DO 1002 I=1,N
      DO 1002 J=1,3
 1002 V(I,J)=((V(I,J)-X(I,J))/DT)*DTN(NT)+X(I,J)
      DO 1003 I=1,M
      DO 1003 J=1,3
      C2(I,J)=(C2(I,J)*DT)/DTN(NT)
 1003 C(I,J)=(C(I,J)*DT)/DTN(NT)
      DT=DTN(NT)
      DDT=DT*DT
      INO1=1
 6003 NT=NT+1
      WRITE (3,4053) T,DT
      GO TO 101
C     TOLERANCE OUTSIDE LIMITS HAS IT BEEN REPEATED
 3002 LL=MOD(K,2)
      IF (LL) 3006,3006,4005
 4005 WRITE (3,4051) T
      GO TO 3005
C     THIS STEP HAS NOT BEEN REPEATED TRY AGAIN
 3006 GO TO 3007
C     FOR CHECK
 3100 WRITE (3,5004)
 5004 FORMAT (22H TOL OVER LIMIT REPEAT)
      GO TO 9041
 9041 CONTINUE
      IF (DT-DTN(NT-1)) 6001,6000,6001
 6001 NT=NT-1
      GO TO 1000
 6000 GO TO 101
C     ODD TIME STEP
 3012 K=K
      EGKA1=ENGKA
      EGPO1=ENGPO
      EGSP1=ENGSP
      EGLO1=ENGLO
      EGTO1=ENGTO
      DSCR1=DESCR
      GO TO 101
 1111 FORMAT (2X,I5)
   70 FORMAT (E15.4,I5,I2,I2,I4,2I5,3E15.4,2I4)
   71 FORMAT (2E15.4,2E15.4)
   72 FORMAT (3E15.4)
   73 FORMAT (E15.4,E15.4,E15.4)
   74 FORMAT (I5,E15.4,E15.4)
   76 FORMAT (3X,I5,I5,I5,I5,E15.4,I5)
   55 FORMAT (2X,I4,2X,3HVX=,E15.4,2X,3HVY=,E15.4,2X,3HVZ=,
     1E15.4)
   75 FORMAT (4E15.4,4E15.4,4E15.4,E15.4,I4)
   81 FORMAT (4(3E15.8),E15.8,I5)
```

```
      END
      SUBROUTINE SETBX
C
C     SET UP BOX AND PLACE AND LOCATE ATOMS
C
C
      INTEGER BOX,BBOX
      COMMON BOX(4096),AC(3),IBND(1000),E(1001),X(1000,3),
     1F3(1001),IAUX(27),IDUX(27),J,L,I,L2,IGAM,BBOX,XX,YY,
     2E2,H,F,ENGPO,ZZ1(1000),ZZ2(1000),ZZ3(1000),A1(3)
     3,F1(1001),EE2(1001),F2(1001),EE3(1001),IMNT,IK(2735),
     4ZZ,RR,E1,B1(3),EE1(1001)
C
      IF (J.GT.4096) GO TO 40
      IF (BOX(J).GT.0) GO TO 10
      BOX(J)=L
      GO TO 30
   10 IF (BOX(J)/1001.GT.0) GO TO 20
      BOX(J)=BOX(J)+1001*L
      GO TO 30
   20 BOX(J)=BOX(J)+1001*1001*L
   30 IBND(L)=J+10000*IBND(L)
      RETURN
   40 CALL EXIT
      END
      SUBROUTINE SRHBX
C
      COMMON BOX(4096),AC(3),IBND(1000),E(1001),X(1000,3),
     1F3(1001),IAUX(27),IDUX(27),J,L,I,L2,IGAM,BBOX,XX,YY,
     2E2,H,F,ENGPO,ZZ1(1000),ZZ2(1000),ZZ3(1000),A1(3)
     3,F1(1001),EE2(1001),F2(1001),EE3(1001),IMNT,IK(2735),
     4ZZ,RR,E1,B1(3),EE1(1001)
C
      INTEGER BOX,BBOX
C
      IMNT=IBND(I)
      IF(IMNT) 690,690,691
  690 IBND(I)=IMNT/10000-1
      J=IMNT-IBND(I)*10000
      L2=0
      GO TO 692
  691 IBND(I)=IMNT/10000
      J=IMNT-IBND(I)*10000
      L2=IABS(IBND(I))
  692 L2=L2+1
      AC(1)=ZZ1(I)
      AC(2)=ZZ2(I)
      AC(3)=ZZ3(I)
      K=IDUX(L2)
      K1=IAUX(L2)-1
      DO 178 KK=1,K
      JJ=J+IK(K1+KK)
      IF (JJ)178,178,131
  131 IF (JJ-IGAM)135,135,178
```

```
135 IF (BOX(JJ))138,178,138
138 BBOX=BOX(JJ)
139 L=MOD(BBOX,1001)
    IF (L-I) 176,176,143
143 XX=X(I,1)-X(L,1)
    IF (ABS(XX)-2.5) 147,147,176
147 YY=X(I,2)-X(L,2)
    IF (ABS(YY)-2.5) 151,151,176
151 ZZ=X(I,3)-X(L,3)
    IF (ABS(ZZ)-2.5) 156,156,176
156 RR=XX*XX+YY*YY+ZZ*ZZ
    IF (RR-6.25) 159,159,176
159 AAA=0.00
    H=(E1*RR+E2)+AAA
    IH=H
    H=H-IH
    IF(RR-1.69)501,502,502
501 IF(RR-.49)503,504,504
502 F=H*(F3(IH+1)-F3(IH))+F3(IH)
    ENGPO=ENGPO+EE3(IH)+H*(EE3(IH+1)-EE3(IH))
    GO TO 512
504 F=H*(F2(IH+1)-F2(IH))+F2(IH)
    ENGPO=ENGPO+EE2(IH)+H*(EE2(IH+1)-EE2(IH))
    GO TO 512
503 F=H*(F1(IH+1)-F1(IH))+F1(IH)
    ENGPO=ENGPO+EE1(IH)+H*(EE1(IH+1)-EE1(IH))
    GO TO 512
512 CONTINUE
    XX=F*XX
    AC(1)=XX+AC(1)
    YY=F*YY
    AC(2)=AC(2)+YY
    ZZ=F*ZZ
    AC(3)=AC(3)+ZZ
    ZZ1(L)=ZZ1(L)-XX
    ZZ2(L)=ZZ2(L)-YY
    ZZ3(L)=ZZ3(L)-ZZ
176 BBOX=BBOX/1001
    IF(BBOX) 139,178,139
178 CONTINUE
    RETURN
181 CALL EXIT
    END
```

Note: The definitions of the variables used in this program are identical to those used by M. Larson((49).

B. Input Data for Computer Program

The following data is needed in part, or in whole, to initiate a dynamic event in the previously presented program.

1. The general starting statistics needed for each program, IPROB,MONTH,KAY,IEAR,IA,IB,IC,NV,NR.
   FORMAT(I5,I2,I2,I4,5I2)
   a. IPROB - problem number.
   b. MONTH - number of the month of the year.
   c. KAY - day of the month.
   d. IEAR - year.
   e. IA,IB,IC - dimensions of the crystal in the X,Y, and Z directions respectively (in units of $\frac{1}{4}$ the Fe_3Al unit cell edge).
   f. NV - the number of vacancies introduced (usually zero).
   g. NR - the number of replacement atoms introduced (usually zero).
2. The coordinates of the vacancies introduced into the lattice (not usually used), INV(K,J),J=1,3, K=1,NV.
   FORMAT(24I3)
3. Data needed for replacement atoms (not usually used), (X(I,J),J=1,3),IBND(I).
   FORMAT(3F15.4,I15)
   a. X(I,J) - the coordinates of each replacement atom with identification number I.

b. IBND(I) - boundary condition of the replacement atom I.

4. Data for calculation of the entries for the single potential function table, AA,BB,RMIN, RMAX.

FORMAT(4E15.4)

a. AA - pre-exponential constant used in calculating potential function.

b. BB - exponential constant.

c. RMIN - minimum separation of two atoms for which the potential interaction is considered.

d. RMAX - maximum separation of two atoms for which the potential interaction is considered.

5. Potential function constants for a combination of three potentials, (A1(I),B1(I),I=1,3).

FORMAT(2F10.6)

a. A1(I) - pre-exponential constants for each of the three potential funtions.

b. B1(I) - exponential constants for each of the three potential functions.

6. Time step increment, DT.

FORMAT(E15.4)

7. Total number of boundary types corresponding to the possible locations of an atom on the surface of the crystallite, M (taken as 26 in all the calculations).

FORMAT(I15)

8. Constants representing the additional forces supplied to the surface atoms of the crystallite, A(I,J),B(I,J),C(I,J).

   FORMAT(3E15.4)

   a. A(I,J) - constant surface force on the atom with identification number I, in the J direction.

   b. B(I,J) - spring constants for surface atoms.

   c. C(I,J) - viscous damping constants for surface atoms (taken as zero in these calculations).

9. Number of initially moving atoms, MOV.

   FORMAT(I15)

10. Coordinates of initially moving particle, XM(J),J=1,3.

    FORMAT(3F15.4)

11. Data needed to identify primary knock-on, L, D(1),D(2),D(3).

    FORMAT(I15,3E15.4)

    a. L - identification number of initially moving particle.

    b. D(1),D(2),D(3) - velocities of initially moving particle in the X,Y, and Z directions respectively.

12. Data for determining the length of the program and time step changes, (TT(I),DTN(I),I=1,6).

    FORMAT(6(F7.2,F5.2))

a. TT(I) - total time that program is to run until terminated or time step changed.

b. DTN(I) - new time step used after the program has run a total time of TT(I) and the time step is being changed from DTN(I-1).

APPENDIX B

Calculation of Constants

A. Calculation of Constant Surface Forces

The spring forces applied to the surface atoms were chosen so as to balance the effects of near and second near neighbor atoms just below the surface of the crystallite. At normal equilibrium separations this surface force must be calculated from the derivative of the Morse potential:

$$\phi(r) = D\{\exp[-2\alpha(r-r_o)] - 2\exp[-\alpha(r-r_o)]\} \quad (1)$$

where,

$D=0.6205$ eV $\alpha = 1.628$ unit^{-1} $r_o = 2.000$ units

and the unit of length is one half the unit cell edge of Fe_3Al (see Appendix C).

The derivative of the interaction potential with respect to r gave the force between two atoms separated by a distance "r".

$$F(r) = \frac{d\phi(r)}{dr} = D\{-2\alpha\exp[-2\alpha(r-r_o)] + 2\alpha\exp[-\alpha(r-r_o)]\} \quad (2)$$

with the constants the same as given above. Having considered only first and second near neighbor contributions the resultant normal force was seen to be:

$$F_n = F(2) + 4F(\sqrt{3}) * 1/\sqrt{3} \quad (3)$$

so that from equation 2:

$$F(2) = D\{-2\alpha\exp[-2\alpha(2.0-2.0)] + 2\alpha\exp[-\alpha(2.0-2.0)]\}$$

or

$$F(2) = 0$$

and

$$F(\sqrt{3}) = D\{-3.256\exp[-3.256(1.732-2.000)] + 3.256\exp[-1.628*(1.732-2.000)]\}$$

or

$$F(\sqrt{3}) = -1.707(\text{eV unit}^{-1})$$

The total normal force was then found from equation 3.

$$F = 0 + 4*(-1.707)*1/\sqrt{3} = 3.950(\text{eV unit}^{-1})$$

In the computer calculations the spring force was carried as 1/2000 the force calculated above so that the mass of the atoms would not need to be considered (see unit mass, Appendix C).

B. Calculation of Spring Constants for Surface Atoms

The spring constants used in this program were calculated in the manner described by Gibson, et al. (35) for F.C.C. copper. The cubic crystallite was first replaced by a sphere of equal volume assumed to be surrounded by an infinite isotropic homogeneous elastic medium. This sphere was then allowed to expand from a radius of R to R+dR, such that the elasticity equations predicted a surface pressure proportional to the displacement of the surface dR of:

$$P = (4\mu/R)\, dR \qquad (4)$$

where μ was the shear modulus of the medium; equal to C_{44} in these calculations. The effective normal spring

constant was then found by dividing P by the total number of atoms per unit area of the original cube face. Since the constant was proportional to dR, the spring constant was taken to be the force per unit surface displacement, dR. The computations were done as follows:

Volume of sample crystallite (12x12x12 in units of 1/4 Fe_3Al unit cell edge):

$$Vc=(e)^3=(12)^3=1728 \text{ units}^3$$

Volume of equivalent sphere:

$$Vs=4/3\pi R^3=1728 \qquad R=10.9 \text{ units}$$

From Leamy (48) C_{44} for Fe_3Al was found to be:

$$C_{44}=1.303 * 10^{12} \text{ dynes/cm}^2$$

and from equation (4):

$$P=\frac{4(1.303*10^{12})}{10.9}dR = \qquad dR=4.76*10^{11} \frac{\text{dynes}}{\text{cm}^2 \text{ unit}}$$

The total surface area of the cube was:

$$A=12*12*6=864 \text{ units}^2$$

The total number of surface atoms in this array was 220, so that the number of atoms per unit area was:

$$\text{Number per unit area}=\frac{220}{864}=.2555$$

and from this the pressure per atom was calculated to be:

$$P=\frac{4.76*10^{11}}{.255} = 1.795*10^{12}$$

and after changing units the final value was arrived at for the normal spring constant on a surface atom (divided again by 2000 to eliminate mass considerations).

$$k_n=2.02*10^{-3} \text{ eV/unit}$$

and

$F_n = K_n dR$

By employing the concept of a cylindrical crystallite, Gibson, et al. (35) indicated that the tangential spring constant, k_t, could be found from the relation:

$k_t = 1/4 k_n$

so that,

$k_t = 5.05 * 10^{-3}$ eV/unit.

APPENDIX C

Units Used in Computer Calculations

The basic unit of length was taken to be 1/4 the Fe_3Al unit cell edge:

$$l_o = 1.000 \text{ unit} = 1.3250^{\circ}A$$

the unit of time was considered so that a 1000 eV aluminum atom would have unit velocity,

$$t_o = 3.432*10^{-15} \text{sec.}$$

the unit of energy was taken to be one electron volt or:

$$E_o = 1.602*10^{-12} \text{erg}$$

and the unit velocity was:

$$v_o = 8.46*10^{6} \text{ cm/sec.}$$

The unit mass was calculated to be 1/2000 the mass of the aluminum atom, or:

$$m_o = 2.240*10^{-26} \text{gm.}$$

APPENDIX D

TABLE OF COMPUTER RUNS

Run Number	Direction of Knock-on	Number	Type	Coordinates	Energy	Final Time	Remarks
1	[100]	280	Fe	6,6,6	46eV	35	A series of replacement collisions was initiated that soon extended past the boundary of the crystal.
2	[100]	110	Fe	2,6,6	46eV	40	A series of replacement collisions with vacancy formed at initial location of knock-on and interstitial several unit distances away.
3	[100]	110	Fe	2,6,6	32eV	46	Replacement chain with fewer replacements than above; above threshold.
4	[100]	110	Fe	2,6,6	25eV	42	Replacement chain barely initiated; just above threshold.
5	[100]	110	Fe	2,6,6	21eV	35	Knock-on not displaced permanently; below threshold energy.
6	[111]	143	Al	3,3,5	43eV	54	Aluminum atom oscillates in potential well of initial location; below threshold.
7	[111]	143	Al	3,3,5	47eV	59	Same as No. 6, but with more motion.
8	[111]	143	Al	3,3,5	50.7eV	60	Still no permanent displacement of the Al atom; below threshold.

APPENDIX D (cont'd)

Run Number	Direction of Knock-on	Number	Type	Coordinates	Energy	Final Time	Remarks
9	[111]	142	Fe	3,3,3	39.7eV	60	Unlike normal replacement chain, the atoms further along the chain were displaced more than those at the beginning; below threshold.
10	[111]	142	Fe	3,3,3	50eV	60	Same result as No. 9, only more extended.
11	[111]	94	Fe	2,2,2	56eV	70	Same as Nos. 9 and 10 with more motion. Aluminum atoms oscillate in their potential wells. Below threshold.
12	[111]	187	Fe	4,4,4	59eV	70	Still no permanent displacements.
13	[111]	94	Fe	2,2,2	89.4eV	62	Replacement collisions not initiated with knock-on, but several unit lengths along the collision chain. Motion of Al atoms very significant.
14	[110]	144	Fe	3,3,7	23.3eV	32	No permanent displacement; below threshold.
15	[110]	144	Fe	3,3,7	33.5eV	70	Same as No. 14.
16	[110]	144	Fe	3,3,7	23.3eV	37	Test to see if event was already above threshold.

APPENDIX D (cont'd)

Run Number	Direction of Knock-on	Number	Type	Coordinates	Energy	Final Time	Remarks
17	[110]	144	Fe	3,3,7	50eV	42	Single replacement formed just past knock-on. Split interstitial formed by the knock-on and first replaced atom; above threshold.
18	[110]	144	Fe	3,3,7	41.4eV	42	No permanent displacement; below threshold. Focusons drew energy away from collision chain.
19	[110]	144	Fe	3,3,7	50eV	66	Same as No. 18. Trying for stable equilibrium.
20	[110]	144	Fe	3,3,7	50eV	152	Run to stability of "split-interstitial."
21	[110]	143	Al	3,3,5	39eV	60	Below threshold, with same results as for the Fe knock-on.
22	[110]	143	Al	3,3,5	46.2eV	60	Just above threshold.
23	[110]	143	Al	3,3,5	51.2eV	60	Well above threshold to check on No. 22. Results very similar to iron knock-on.
24	1.5° from [100]	110	Fe	2,6,6	109eV	60	Gross defocusing in the direction of Al near neighbors.

APPENDIX D (cont'd)

Run Number	Direction of Knock-on	Number	Type	Coordinates	Energy	Final Time	Remarks
25	1.5° from [100]	155	Al	3,7,5	105eV	60	Gross defocusing, especially at Al atoms. Al knock-on not permanently displaced.
26	1.0° from [111]	142	Fe	3,3,3	107eV	60	Gross defocusing, especially at Al atoms. Extensive lattice expansion near end of collision chain.

BIBLIOGRAPHY

1. TAMMANN, G. (1919) Z. Anorg. Allgem. Chem., 107, p. 1.

2. JOHANSSON, C.H. and J.O. LINDE (1925) Ann. Physik, 78, p. 439.

3. REED-HILL, R.E. (1964) Physical Metallurgy Principles. D. Van Nostrand Company, Inc., New York, p. 341-346.

4. DARKEN, L.S. and R.W. GURRY (1953) Physical Chemistry of Metals. McGraw-Hill Book Company, Inc., New York, p. 92-102.

5. HANSEN, M. and K. ANDERKO (1958) Constitution of Binary alloys. McGraw-Hill Book Company, New York.

6. BRADLEY, A. and A. JAY (1932) Proc. Roy. Soc., A136, p. 210.

7. MOTT, N.F. and H. JONES (1936) The Theory of the Properties of Metals and Alloys. Oxford University Press, London, p. 29-31.

8. DIENES, G.J. and G. H. VINEYARD (1957) Radiation Effects in Solids. Interscience Publishers, Inc., New York, p. 82-83.

9. BILLINGTON, D.S. and J.H. CRAWFORD (1961) Radiation Damage in Solids. Princeton University Press, Princeton, New Jersey, p. 13-14, 37-53, 171-181.

10. KINCHIN, G. H. and R.S. PEASE (1955) Journal of Nuclear Energy, 1, p. 200.

11. BILLINGTON, D.S. and J. H. CRAWFORD (1961) Radiation Damage in Solids. Princeton University Press, Princeton, New Jersey, p. 37-53.

12. LEIBFRIED, G. (1959) Journal of Applied Physics, 30, p. 1388.

13. LEIBFRIED, G. (1964) The Interaction of Radiation with Solids, Proceedings of the International Summer school on Solid State Physics held at Mol, Belgium, August 12-31, 1963, North Holland Publishing Company, Amsterdam, p.1.

14. BRINKMAN, J.A. (1954) Journal of Applied Physics, 25, p. 961.

15. SEITZ, F. (1949) Disc. Faraday Soc., 5, p. 271.

16. SEITZ, F. and J.S. KOEHLER (1956) Solid State Physics, 2, p. 305.

17. SILSBEE, R.H. (1957) Journal of Applied Physics, 28, p. 1246.

18. KAYA, S. and A. KOSSMAN (1931) A. Physik, 72, p.293.

19. SIMPSON, A.W. and R.H. TREDGALD (1954) Proc. Phys. Soc., 1367, p. 38.

20. SEIGEL, S. (1949) Effects of neutron bombardment on order in the alloy Cu_3Au. Phys. Rev., 75, p. 1823.

21. DIENES, G.J. and G.H. VINEYARD (1957) Radiation Effects in Solids. Interscience Publishing Co., New York.

22. BRINKMAN, J.A., C.E. DIXON, and C.J. MEECHAN (1954) Interstitial and vacancy migration in Cu_3Au and copper, Acta Met., 2, p.38.

23. THOMAS, D.E. (1956) Irradiation effects on physical metallurgy processes, IMD Special Report Series No. 3, Nuclear Metallurgy, AIME, New York, Vol. 3, p. 13-31.

24. WALKER, R.M. (1960) Journal of Nuclear Materials, No.2, p. 147.

25. PUGH, S.F. (1964) The Interaction of Radiation with Solids, Proceedings of the International Summer School on Solid State Physics held at Mol, Belgium, August 12-31, 1963, North Holland Publishing Company, Amsterdam, p. 261.

26. DUGDALE, R.A. (1956) Phil. Mag., 1, p. 537.

27. RUDMAN, P.S. (1962) Acta Meta., 10, p.195.

28. SEIGEL, S. (1949) Phys. Rev., No. 75, p. 1823.

29. COOK, L.G. and R.L. CUSHING (1953) Acta Met., No. 1, p.539, p. 549.

30. BLEWITT, T.H. and R.R. COLTMAN (1952) Phys. Rev., No. 85, p. 384.

31. BRINKMAN, J.A. and C.E. DIXON and C.J. MEECHAN (1954) Acta Meta., No. 2, p. 38.

32. BETTS, B. (1968) Private Communication

33. SAENKO, G.P. (1962) Effects of neutron irradiation on the ordered alloy Fe_3Al. U.S.A.E.C. Report, ADC*TR*5245, p. 15.

34. TOMA, ROBERT F. (1965) A Study of Order-Disorder in Fe_3Al at Various Temperatures Induced by Neutron Irradiation, Rolla, Missouri. Thesis, University of Missouri at Rolla.

35. GIBSON, J.B., A.N. GOLAND, M. MILGRAM, and G.H. VINEYARD (1960) Dynamics of Radiation Damage, Phys. Rev., Vol. 120, No. 4, p. 1229-1253.

36. BEELER, J.R., JR. (1965) Flow and Fracture of Metals and Alloys in Nuclear Environments, ASTM Special Technical Publication No. 380, p. 86-103.

37. HOLMES, D.K. and G. LEIBFRIED (1960) Range of Radiation Induced Primary Knock-ons in the Hard Core Approximation, Phys. Rev., Vol. 31, No. 6, p.1046-1056.

38. HUNTINGTON, H.B. (1953) Mobility of Interstitial Atoms in a Face-Centered Metal, Phys. Rev., Vol. 91, No. 5, p. 1092-1098.

39. JOHNSON, R.A. and E. BROWN (1962) Point Defects in Copper, Phys. Rev., Vol 127, No. 2, p. 446-454.

40. TEWORDT, LUDWIG (1958) Distortion of the Lattice Around an Interstitial, a Crowdion, and a Vacancy in Copper. Phys. Rev.,Vol.169, 1,p.81.

41. HUNTINGTON H.B. and SEITZ (1942), Phys. Rev., Vol. 61, p. 315.

42. VINEYARD, G.H. (1962) Radiation Damage in Solids, Proceedings of the International School of Physics "Enrico Fermi", Academic Press, New York, p. 291.

43. ERGINSOY, C., G.H. VINEYARD, and A. ENGLERT (1964) Dynamics of Radiation Damage in a Body Centered Cubic Lattice, Phys. Rev., Vol 133, No. 2A, p. A595-A606.

44. VINEYARD, G.H. (1963) J. Phys. Soc. Japan, Vol. 18, Supplement III, p. 144.

45. RUDMAN, P.S. (1967) Intermet allic Compounds, Edited by J.H. Westbrook, John Wiley and Sons, Inc., New York, p. 405-425.

46. VINEYARD, G.H. (1968) Private Communication.

47. GIRFALCO, L.A. and V.G. WEIZER (1959) Application of Morse Potential Function to Cubic Metals, Phys. Rev., Vol. 114, No. 3, p. 687-690.

48. LEAMY, H.J. (1967) The elastic Stiffness Coefficients of Iron-Aluminum Alloys-ii The Effect of Long Range Order, Acta Metallurgica, Vol. 15, No. 12, p. 1839-1851.

49. LARSON, A. (1964) Grape-A Computer Program for Classical Many-Body Problems in Radiation Damage, BNL-7979.

VITA

The author was born on December 16, 1944, in St. Louis, Missouri. He graduated from Southwest High School, St. Louis, Missouri, in January, 1963.

He received his Bachelor or Science Degree in Metallurgical Engineering with a Nuclear Option in May, 1967, from the University of Missouri at Rolla.

The author entered graduate school in the Nuclear Engineering Department at University of Missouri at Rolla in September, 1966, and was granted an AEC Traineeship starting in January of 1967.

The following summer, August of 1967, the author was married and returned with his wife to school in the fall of 1967 to continue his research.